AD-A111 135 AIR FORCE INST OF TECH WRIGHT-PATTERSON AFB OH SCHOO--ETC F/G 20/2
PHOTOLUMINESCENCE STUDY OF ION IMPLANTATION DAMAGE IN GALLIUM A--ETC(U)
DEC 81 M V KEY
UNCLASSIFIED AFIT/GEO/PH/81-2 NL

1 OF 1
AD
A111135

END
DATE
FILMED
3-82
DTIC

① LEVEL II

DISTRIBUTION STATEMENT A
Approved for public release;
Distribution Unlimited

DEPARTMENT OF THE AIR FORCE
AIR UNIVERSITY (ATC)

AIR FORCE INSTITUTE OF TECHNOLOGY

Wright-Patterson Air Force Base, Ohio

82 02 18 065

AFIT/GEO/PH/81-2

(1) LEVEL II

PHOTOLUMINESCENCE STUDY OF ION IMPLANTATION DAMAGE IN GALLIUM ARSENIDE

THESIS

AFIT/GEO/PH/81-2 Manuel V. Key
Captain USAF

Approved for public release; distribution unlimited

AFIT/GEO/PH/81-2

PHOTOLUMINESCENCE STUDY OF ION IMPLANTATION DAMAGE IN GALLIUM ARSENIDE

THESIS

Presented to the Faculty of the School of Engineering
of the Air Force Institute of Technology
Air University
in Partial Fulfillment of the
Requirements for the Degree of
Master of Science

by

Manuel V. Key, B.S.
Capt USAF

Graduate Electro-Optics

December 1981

Approved for public release; distribution unlimited

Preface

The completion of this thesis was a very gratifying and educational experience. It provided valuable exposure to topics which were heretofore relatively foreign to me, such as photoluminescence processes and cryogenic techniques. It also provided further practical experience in other optical diagnostic methods covered in the related course work.

My appreciation is most gratefully extended to my advisor, Dr. Robert L. Hengehold, for his patience and advice throughout this effort. I would also like to thank the sponsoring organization, the *Avionics Laboratory* (AFWAL/AADR, Dr. Y. S. Park), for providing the samples necessary for this study. The personal interest taken by Captain Gernot Pomrenke, of that organization, was also greatly appreciated. Additional thanks go to Jim Miskimen, Ron Gabriel, and George Gergal of the AFIT Physics Laboratory staff for their technical assistance. My appreciation is finally extended to my family, whose active moral support was of great comfort during this trying period.

Manual V. Key

This thesis was typed by Phyllis Reynolds.

Contents

Page

List of Figures

Figure Page

List of Tables

Table Page

Abstract

The 5° photoluminescence (PL) from 1.55 eV to 1.36 eV of semi-insulating bulk GaAs implanted with Si was observed, using the 488 nm line of an argon-ion laser. Implant dosages were 10^{12}, 10^{13}, 10^{14}, and 10^{15} ions/cm^2. Separate sets of samples were annealed at 750°C and 900°C. The virgin unannealed sample spectrum contained a shallow donor peak at 1.513 eV, a carbon donor-to-carbon acceptor peak at 1.490 eV, a possible carbon donor-to-zinc acceptor peak at 1.487 eV, and an optical phonon peak at 1.454 eV. The virgin annealed sample spectra included, additionally, a vacancy complex-to-silicon acceptor peak at 1.406 eV, a Ga vacancy complex peak at 1.358 eV and a phonon replica at 1.322 eV. The spectra of the implanted unannealed samples showed an increasing quenching of native peaks with increasing dosage, and included no new damage related peaks. The spectra of the implanted samples showed an increase in the native peaks due to annealing but not due to Si dosage increases. The increase in Si dosage caused an increase in low energy broad peaks. A temperature study (5°K to 77°K), and chemical etching depth resolved study of a sample implanted with 10^{15} ions/cm^2 and annealed at 900°C showed two broad peaks: one near 1.38 eV and one near 1.42 eV. The peaks were seen to vary inversely with

temperature in amplitude only; but as etch depth increased, the amplitudes increased then decreased, finally disappearing at an etch depth of 0.2 microns. The peaks were attributed to complex centers associated with Si in As sites and As vacancies. A similar study using chemical etching followed by a measurement of normalized PL of the 1.49 eV peak in the unannealed samples, showed that the PL was not restored to that of the virgin sample until nearly twice the damage depth predicted by LSS theory was reached. This was attributed to the diffusion of defects during the room temperature implantation process.

PHOTOLUMINESCENCE STUDY OF ION IMPLANTATION DAMAGE IN GALLIUM ARSENIDE

I. Introduction

Background

The United States Air Force has, for the past decade, been involved in research efforts to identify, develop, and implement new semiconductor materials more suited to defense applications than those previously developed by industry for the civilian consumer. Several new device applications, primarily in the microwave area, depend on the development of such new materials. The requirement for this new technology was derived from the need for increased signal processing speed in electronic warfare, nuclear hardening of critical components, new real-time digital radar systems, and the need to expand and improve satellite reconnaissance and communication systems (Ref 1). The Electronics Research Branch of the Air Force Avionics Laboratory (AFWAL/AADR) has been providing research in this area, and, for the past several years, has devoted a large portion of its efforts to the study of gallium arsenide (GaAs) (Refs 1:33; 2:1).

Gallium arsenide is a group III-V semiconductor compound that has experimentally demonstrated characteristics which are very well suited to some of the new device applications. It possesses a relatively wide direct band gap of 1.435 eV at 294°K, which reduces its vulnerability to radiation damage. Also, it has a high electron mobility and a short minority career lifetime (Ref 3:325), which greatly increase its signal processing speed.

Unfortunately, efforts to establish reliable manufacturing techniques have encountered many problems. Many of these problems arise during doping in the device manufacturing stage. For instance, doping using the diffusion method requires the material to be at elevated temperatures; which, because of arsenic's high vapor pressure, causes the material to badly decompose. Therefore, many researchers have adopted the method of ion implantation for introducing electrically or optically active ion species into semiconductors. This technique has been successfully used in the production of bipolar and field effect transistors, integrated circuits, microwave devices, and optoelectronic devices (Ref 4:627). One major advantage of this method over the dopant diffusion technique is that it can be performed at room temperature. Although annealing of the samples is necessary to activate the dopant ions, the annealing temperatures are much lower than those of the diffusion method. Although ion implantation offers this and other advantages, some of which are discussed in Chapter II, it has one major drawback. The collisions of the implanted ions with the atoms of the host lattice produce atomic displacement damage, which, in some cases, destroys the original beneficial effects of doping. Although several studies have been made (Refs 4; 5; 6; 7), and techniques devised to characterize the damage profile, and the microscopic mechanisms causing it; a detailed understanding has not yet been gained.

Photoluminescence is a non-destructive optical diagnostic technique which can be used to evaluate the composition as well as the crystalline quality of the semiconductor device. The process relies on the radiative recombination of electron-hole pairs of a material excited by photons. The technique's sensitivity to crystal lattice disruptions as well as the simplicity it offers in gathering data, make it ideally suited to studies of lattice damage.

Purpose and Scope

The purpose of this study was to investigate the damaging effects of ion implantation in gallium arsenide using photoluminescence as the primary diagnostic tool. Fifteen sets of samples were generated by varying the implant dosage and annealing temperature. Only silicon was used as an implant species. The surface photoluminescence of all the samples was measured to determine the more likely candidates for further investigation. Once this was done, the sample's photoluminescence intensity was measured after successive layers of the material were removed by chemical etching. The magnitude of the resultant photoluminescence intensity as a function of sample depth was used as an indication of crystal lattice damage caused by ion implantation. Because of recent advances and renewed interest in semi-insulating bulk grown crystals, this type of material was used throughout the experiment.

II. Theory

Since this effort is primarily concerned with the damaging effects of ion implantation in gallium arsenide, it is necessary to discuss the basic theory needed to understand the procedures and results of this experiment. This chapter contains a discussion of basic semiconductor band theory, photoluminescence theory and ion implantation.

Semiconductor Band Theory

A semiconductor is a crystalline material containing an energy band structure in which a band of electronic states, which is completely filled at absolute zero (valence band), is separated by an energy gap from another band which is empty at that temperature (conduction band). This band structure is depicted schematically in Fig. 1(a) (Ref 8:257). Although population within the energy gap is forbidden for a pure material, electrons may transition from the lower energy band to the higher and vice versa if energy greater than the energy gap is absorbed or lost respectively. Fig. 1(b) shows a pure semiconductor at room temperature. The void or hole that a transitioning electron leaves in the valence band has an effective mass and contributes to the conductivity of the material (Ref 9:231).

Pure or intrinsic semiconductors have very low conductivities (Ref 8:260), so they are doped with impurities

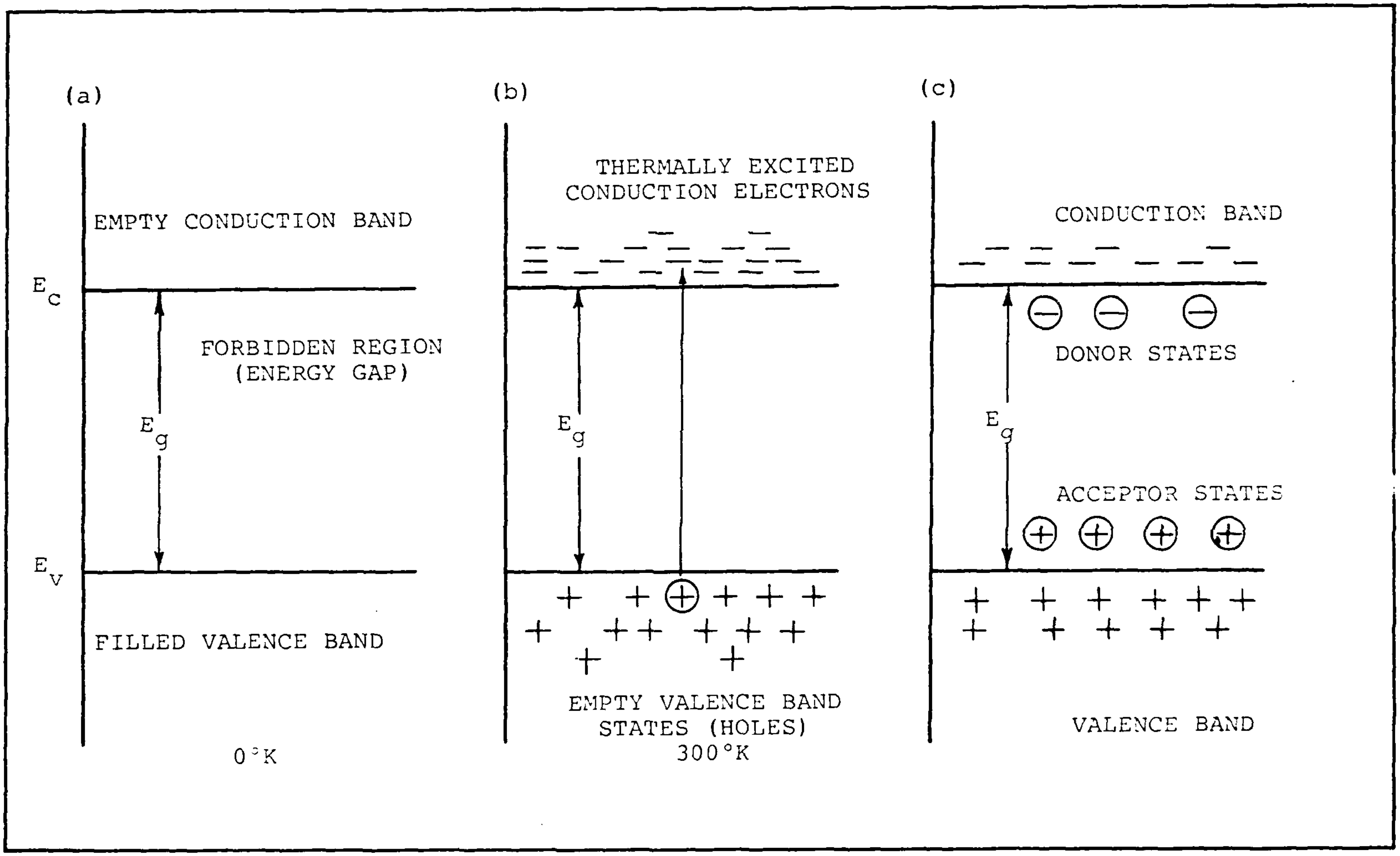

Fig. 1. Conduction and Valence Bands of a Pure Semiconductor, (a) (b); Impurity Levels in a Doped Semiconductor, (c)

in very carefully controlled amounts. The specific type of semiconductor material and type of impurity determine if the impurity becomes an acceptor (p-type) or a donor (n-type). A donor impurity will produce a new electronic state just below the conduction band, and an acceptor will produce one just above the valence band. These new energy levels are schematically depicted in Fig. 1(c).

Usually, when impurities are introduced, they replace constituent atoms, and are referred to as substitutional impurities. For example, in GaAs, a tellurium atom in the arsenic site becomes a donor, as does silicon in the gallium site; since they provide the crystal with more electrons than the atoms they replace. Similarly, a zinc impurity in the gallium site, or silicon in the arsenic become acceptors. A missing atom (vacancy) deprives the crystal of one electron per broken bond; making it an acceptor. An impurity occupying a space between constituent atoms (interstitial) becomes a donor since its outer shell of electrons becomes available for conduction (Ref 10:8).

The recombination of electrons and holes responsible for transitions are categorized into two types, simple and complex centers. In GaAs, a simple center is defined as an impurity which sits on the Ga or the As lattice site and which contributes only one additional carrier to the binding. It is similar to hydrogen in that only the s electrons take part in the binding. Complex centers produce levels that are too broad and too low in energy to be modeled by the hydrogen atom. These deep levels occur in nearly all melt-grown crystals of n-type GaAs even at low doping levels. In p-type GaAs, complex centers are relatively rare (Ref 11:327,359).

Photoluminescence

Photoluminescence (PL) is the optical radiation emitted by a physical system (over and above the thermal equilibrium blackbody radiation) resulting from excitation to a nonequilibrium state by irradiation with light. The process takes place in three distinguishable steps: (i) creation of an electron-hole pair by the absorption of the exciting light, (ii) radiative recombination of electron-hole pairs, and (iii) escape of the recombination radiation from the system. The greatest excitation of the sample takes place near the surface with the resulting carrier distribution being both inhomogeneous and nonequilibrium. To regain homogeneity and equilibrium, the carriers diffuse away from the surface while being depleted by both radiative and nonradiative processes. Since this recombination radiation is subject to self-absorption, most of the excitation of the crystal is limited to a region within one diffusion length of the material. It also follows that the recombination radiation most readily departs through the illuminated surface (Ref 12:182).

The return to equilibrium of the irradiated sample can take place by either a radiative recombination, nonradiative recombination, or a combination of the two.

Radiative Transitions

During radiative transitions a photon is emitted when an electron drops from an upper to a lower energy level. These levels may be either intrinsic band states or impurity levels (Ref 13:1). Of interest to this study are transitions involving excitons, band to impurity levels, donor to acceptor pairs, and phonon replicas. Fig. 2 depicts these different types of transitions in relation to the conduction and valence bands.

Excitons. Excitons are classified into two categories, free excitons and bound excitons. A free exciton consists of a free hole and a free electron bound by coulomb interaction which are free to move around in the crystal lattice. Their mobility is somewhat reduced since it is associated with a mobile pair rather than with a single particle. Since an exciton has a reduced mass which is lower than that of the electron, the exciton binding energy is smaller than either the donor or acceptor binding energies. Additionally, the exciton states do not have a well defined potential in the semiconductor's energy diagram. However, it is customary to place these states very near the conduction-band edge (Ref 10:12). Because of their unstable nature, free excitons have a very short lifetime, and soon recombine

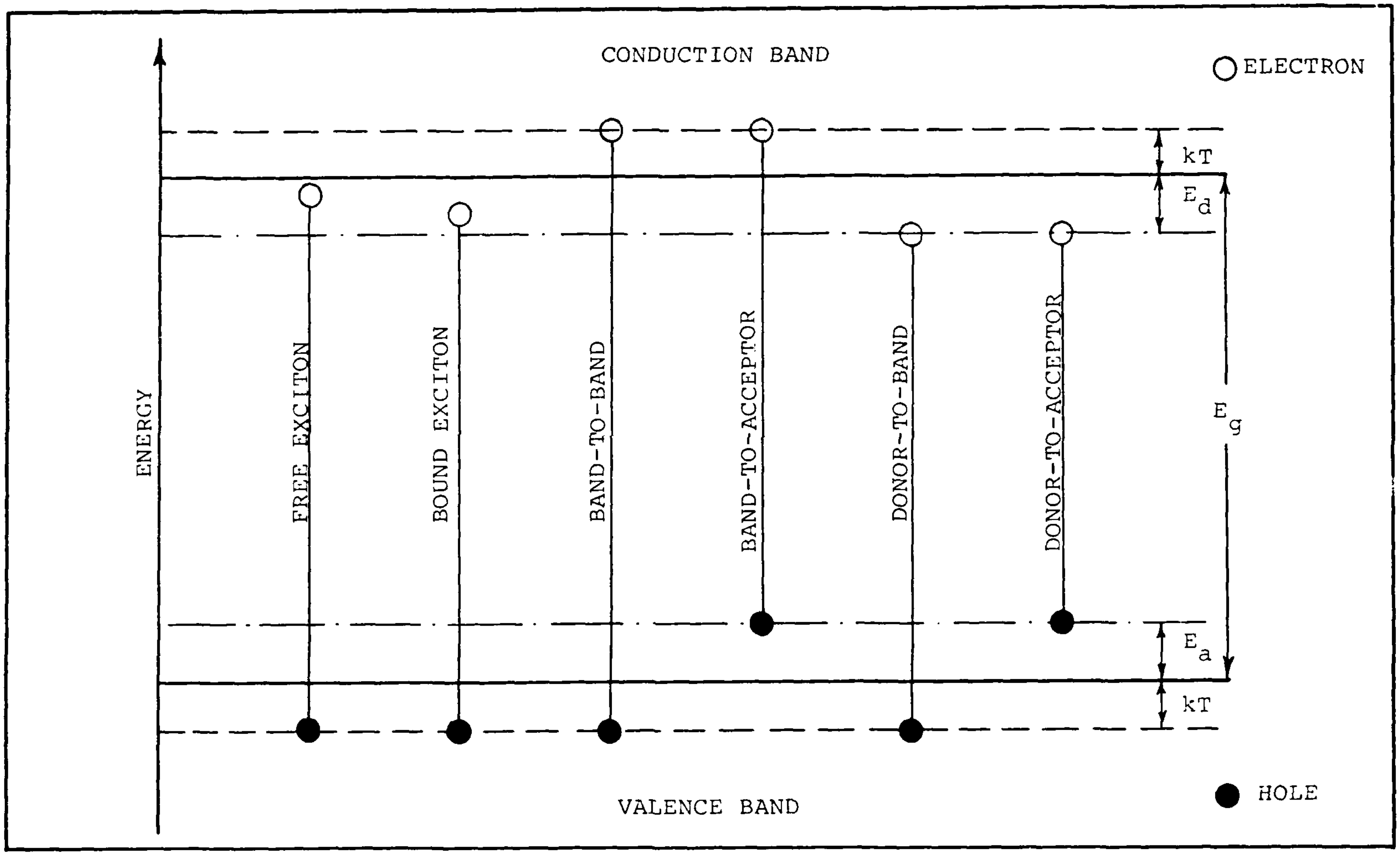

Fig. 2. Radiative Transitions

to emit a photon. In the case of GaAs this radiation can be observed at 1.5156 eV (Ref 11:342). But, since extrinsic transition compete very effectively with excitons in emission, photoluminescence is not observed at these energies unless a high-purity material is used (Ref 12:277).

In certain cases the binding energy of the exciton is increased by the presence of a point defect; for example, a neutral or ionized impurity. Since energy is the main factor that determines whether or not an exciton can be trapped by an impurity, if the total energy of the system is reduced (corresponding to an increase of the binding energy of the exciton) when an exciton is near an impurity, then it becomes energetically favorable for it to remain in that vicinity. The exciton is then said to be "bound" to that impurity (Ref 12:299). The following bound exciton transitions have been observed in GaAs: exciton bound to a neutral donor (1.5145 eV), exciton bound to an ionized donor (1.5133 eV), and exciton bound to a neutral acceptor (1.5125 eV) (Ref 11:342). Different donors and acceptors will result in small shifts in the bound exciton energy position.

Band-to-Impurity Transitions

Band-to-impurity or free-bound transitions involve the recombination of a free electron (hole) with a hole (electron) that is bound to an impurity. The most likely and prominent of the two is the transition between the conduction band and a bound acceptor. Acceptor ionization energies for different elements differ from each other enough to allow the identification of most impurity species with relative ease. The typical energy levels of this type of transition in GaAs for several elements have been reported (Ref 14:1051), and are shown in Table 1.

TABLE 1

TYPICAL CONDUCTION BAND TO BOUND ACCEPTOR TRANSITIONS (Ref 14)

Acceptor	Transition Energy eV
Carbon	1.4935
Silicon	1.4850
Germanium	1.4790
Tin	1.3490
Zinc	1.4888
Cadmium	1.4848
Beryllium	1.4915
Magnesium	1.4911

Since, in GaAs, all donor impurity levels reside in close proximity, and transitions from these levels to the valence band are very weak, they are extremely hard to detect and resolve. However, a very weak line has been observed for most donors near 1.5137 eV (Ref 11:331). Experimental observations of radiative transitions between impurity levels and the more distant band edge are limited to semiconductors with relatively low impurity concentrations (Ref 10:134). As the impurity concentration increases impurity bands begin to form and may eventually merge with the intrinsic bands. This causes the PL peaks to broaden, and makes element identification ambiguous. Shallow transitions from the valence band to an acceptor or from a donor to the conduction band, to neutralize ionized acceptors or donors respectively, are conceivable and could be radiative in the far infrared (Ref 10:131).

Donor-Acceptor Pair Transitions

Another important recombination mechanism involves the transition of an electron trapped on a donor to a hole trapped on an acceptor. When the two form a pair, the normal ionization energy of an isolated donor (or acceptor) is reduced due to the coulombic interaction between the bound electron and hole. If the impurities are substitutional this ionization energy is influenced by the discrete nature of the statistical arrangement of the donors and acceptors within the lattice (Ref 11:335). Thus a numerous series of sharp lines may be observed, each line corresponding to discrete incremental separation of the pair within the crystal lattice. In GaAs, these sharp lines will not be observed for hydrogenic centers (donor-acceptor pairs separated by less than the effective Bohr radius) because their activation energies are so small (Ref 3:10).

At large distances between pair members (distances greater than 40Å), the emission lines overlap, forming a broad spectrum. This is the type of spectrum often observed in GaAs (Refs 10:143-147; 15:1000).

The following are observed characteristics of PL spectra due to donor-acceptor pair recombination (Ref (11:336).

1. Shift of the line to higher energies as the excitation intensity is increased.

2. Appreciable narrowing of the emission band as intensity increases.

3. A band shift towards higher energies with increasing donor concentration.

4. A rapid decrease in intensity as temperatures increase from 25 to 35°K.

5. A shift to higher energies as the temperature increases from 25 to 35°K.

Phonon Coupling. As the binding energy of carriers bound to substitutional impurities increases, the interaction of the carriers with lattice vibrations also increases. When recombination radiation is assisted by these interactions (phonon couplings), the radiation energy is reduced by 36 meV (for longitudinal optical phonons) times the number of phonon assists (Ref 11:388). Most transitions involving acceptors in GaAs may allow phonon assistance, which appear as peaks on the low energy side, and decrease in amplitude as more couplings take place.

Non-Radiative Transitions

A non-radiative transition is a transition from an upper to a lower energy state without emission of a photon. These non-radiative processes are difficult to identify and study because their occurrence can only be assumed from a reduction in radiative emission efficiency. But several mechanisms are possible.

Multiphonon Emission is similar to that mechanism responsible for phonon replicas except that the entire amount of energy of an excited electron is "coupled away" by lattice interactions. Since the energy of a phonon is much less than that of an excited electron multiple phonons must be generated (Ref 13:6).

Auger Effect. This mechanism occurs when an excited electron transfers the energy it would have radiated to another excited electron. The second electron is then raised to a higher state where it can return to a lower energy state by multiple phonon emission.

Non-Radiative Defects

It is well known that recombination at the surface of a semiconductor is non-radiative. It is suspected that the reason for this is that a quasi-continuum of states is formed which joins the valence and conduction bands allowing purely non-radiative recombination. This surface model can be applied to internal surfaces called defects or inclusions. Electrons and holes which are within a diffusion length from the edge of the defect will be drawn to this trap where they will recombine non-radiatively. This process severely reduces the radiative efficiency around the defect. A cluster of defects or of precipitates (metallic phase) can form, further reducing the luminescence efficiency. If the same number of precipitates aglomerate into a few large clusters, the efficiency will be reduced far less than if a uniform distribution of them is dispersed throughout the material.

Not all defects form recombination centers. In some cases, the mechanical strain created in the area of the defect either widens the energy gap, thus repelling both electrons and holes, or creates a field which separates the electron-hole pairs. In either case, the carriers do not recombine radiatively at that location (Refs 10:164-166; 13:7-8).

Ion Implantation

As mentioned in the introduction, ion implantation has become an established technique for introducing dopant ions into semiconductors. This method offers many advantages over the more conventional doping techniques. For a given target material and ion species, the number and depth distribution of the implanted ions can be simply and accurately controlled by the acceleration voltage and beam current. Also, the implanted area can be very well defined by the beam position and the use of masking techniques. Of great importance, also, is the high purity of the beam, made possible by the mass analysis capabilities of the implant equipment. The process is able to provide uncontaminated beams with a high degree of reproducibility (Ref 4:627).

The implantation process involves the ionization of chosen dopant species, the subsequent discrimination by mass analysis of the single desired ion type, and the eventual acceleration and direction of the ions towards the target crystal. The energetic ions entering the target material will, through collisions with target nuclei and electrons, lose their energy and eventually come to rest. The projection of the penetration distance onto the incidence direction is called the projected range. Since the number of collisions and the amount of energy lost per collision are random, not all ions of a given type will have the same projected range. The impurity depth distribution is found to have a gaussian profile with the peak inside the target material. The projected ranges and standard deviations for many types of incident ions and target crystals have been calculated and tabulated using the theory developed by Lindhard, Scharff and Schiott (LSS theory) (Ref 16). These tables give, among other parameters, the projected ranges and standard deviations as functions of acceleration potential (Ref 17). For example, for silicon implanted into

GaAs at a potential of 120 KeV the projected range is 0.1025 microns with a standard deviation of 0.0510 microns.

As the energetic ions travel through the target crystal, atomic displacement damage is produced by collisions with the host lattice. For such collision, the energy transferred may be great enough to completely displace the host atoms from their lattice sites. The displaced atom then becomes a secondary projectile which may collide with other atoms, creating a cascade effect. This process causes a region of damage around the path of the implanted ion. The damage can be of several types; for example, interstitial atoms, substitutional atoms, vacancies, and combinations of these with impurities. The exact type of defect or defect complex depends on several factors, including the mass and energy of the incident ion, and the mass and energy of the host atom (Ref 4:627-628).

It has been found (Refs 4; 5; 6) that, in GaAs, the introduction of damage reduces photoluminescence efficiency in some types of transitions through competition of non-radiative mechanisms. But it has also been reported that damage through ion implantation has enhanced PL efficiency through the creation of other radiative recombination mechanisms such as donor-gallium vacancy complexes. The above references also report that evidence of damage has been found at depths nearly one order of magnitude greater than the projected range of the implanted ion. As stated in the introduction, it is the purpose of this research to study the depth distribution of implantation damage by using the change in PL intensity of incumbent peaks as well as those peaks created by the damage.

III. Equipment and Procedures

This chapter contains a description of the various components of the experimental setup, as well as the general procedures used to gather data. This information is covered in four sections including the sample environment, illumination optics, signal detection and processing, and general procedures.

Sample Environment

The gallium arsenide samples were housed in a research dewar (Janis, Model DT) which was mounted on a vertically adjustable platform attached to the wall. The dewar, depicted in Fig. 3, consisted of a stainless steel cylindrical body which contained an outer and an inner reservoir. The outer reservoir, with a capacity of three and one-half liters, was filled with liquid nitrogen (LN_2). The inner reservoir, also with a capacity of three and one-half liters contained liquid helium (LHe). Both of the reservoirs were surrounded by vacuum walls which were evacuated by a mechanical vacuum pump (Welch Scientific Co., Model 1397), a diffusion pump (Consolidated Vacuum, Model PMC-115), and an Ultek ion pump. The diffusion pump was connected to the inner baffle and was operated continuously throughout the experiment.

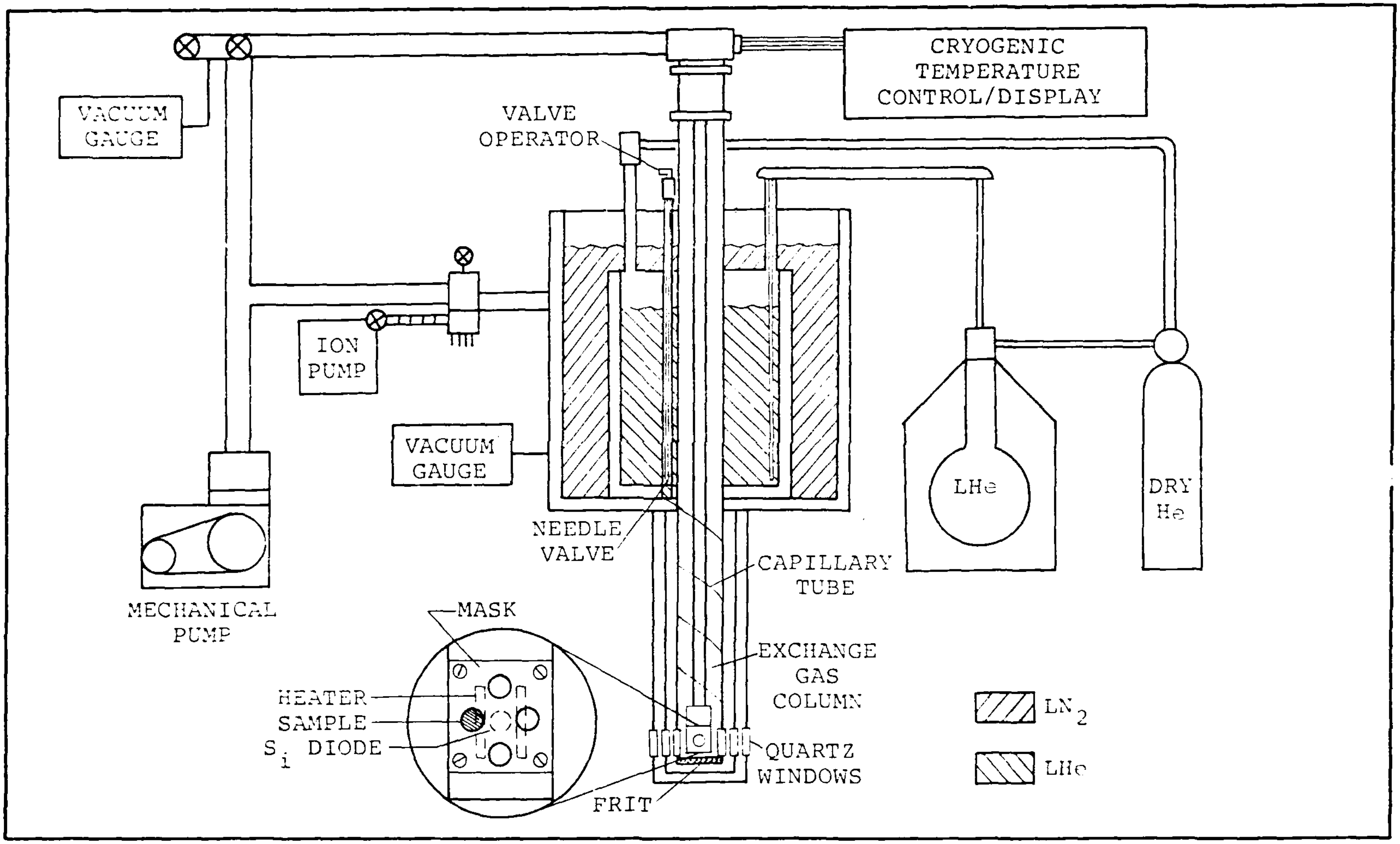

Fig. 3. Sample Environment (Ref. 2)

Liquid helium from the inner reservoir was allowed to flow through a needle control valve to a capillary tube connected to the bottom of the sample chamber. Sample cooling was directly proportional to the LHe flow rate controlled by the valve.

The samples were mounted on the flat area which was cut out of a copper cylinder attached to the end of the sample transfer rod. The samples were held in place by a thin sheet of copper with a hole for each sample, and secured to the copper cylinder by four screws. Mounted directly behind the sample area on the cylinder was a previously calibrated silicon diode which was used as a temperature sensor. Also on the copper mount were three 30 ohm resistive heaters which, together with the silicon diode, were connected to a feedback temperature controller/display (Lakeshore Cryotronics, Model DRC 80C).

Illumination Source and Optics

The GaAs samples were optically excited by the 488.0 nm line of an argon-ion laser (Spectra-Physics, Model 165). This water-cooled laser operated at eight wavelengths ranging from 457.9 nm to 514.5 nm, and had a peak power of 1.1 watts at the 488.0 nm wavelength. The laser's inherent violet/ultraviolet and infrared emissions at all wavelengths necessitated the use of optical filters to purify the output beam. The undesirable infrared emissions were filtered out by using two 90% transmission short-wavelength-pass-filters (see Fig. 4). The first, although possessing a nominal upper cutoff wavelength of 550 nm, could be tuned by varying the incidence angle. An angle of 25° allowed tuning to approximately 489.0 nm. A second filter with a nominal cutoff of 700 nm was added to further attenuate the longer wavelength infrared emissions.

In series with the filters was a spatial filter and beam collimator (Jodon, Model LPSF-100) which was adjusted to expand the beam to approximately 3 cm in diameter. The beam was then turned by a pivoted concave mirror which also focused the beam down to a 16 mm diameter at the sample. Located between the sample chamber and the mirror was a microscope slide which acted as a beam splitter. The reflected part of the beam was directed through a neutral density filter (1.0 O.D.) to a radiometer detector head (EG&G, Model 450-1). The transmitted portion of the beam was directed through the three quartz windows of the sample chamber to the mounted sample. The beam splitter and detector head allowed the continuous monitoring of incident power on the sample throughout each data run. Once the transmissivity of the quartz windows, and the ratio of the transmitted to the reflected power of the beam splitter were experimentally determined, a total ratio of the power at the detector to that incident upon the sample was computed. Then the laser output power was simply adjusted to yield the correct meter reading for the equivalent desired sample illumination. The beam arriving

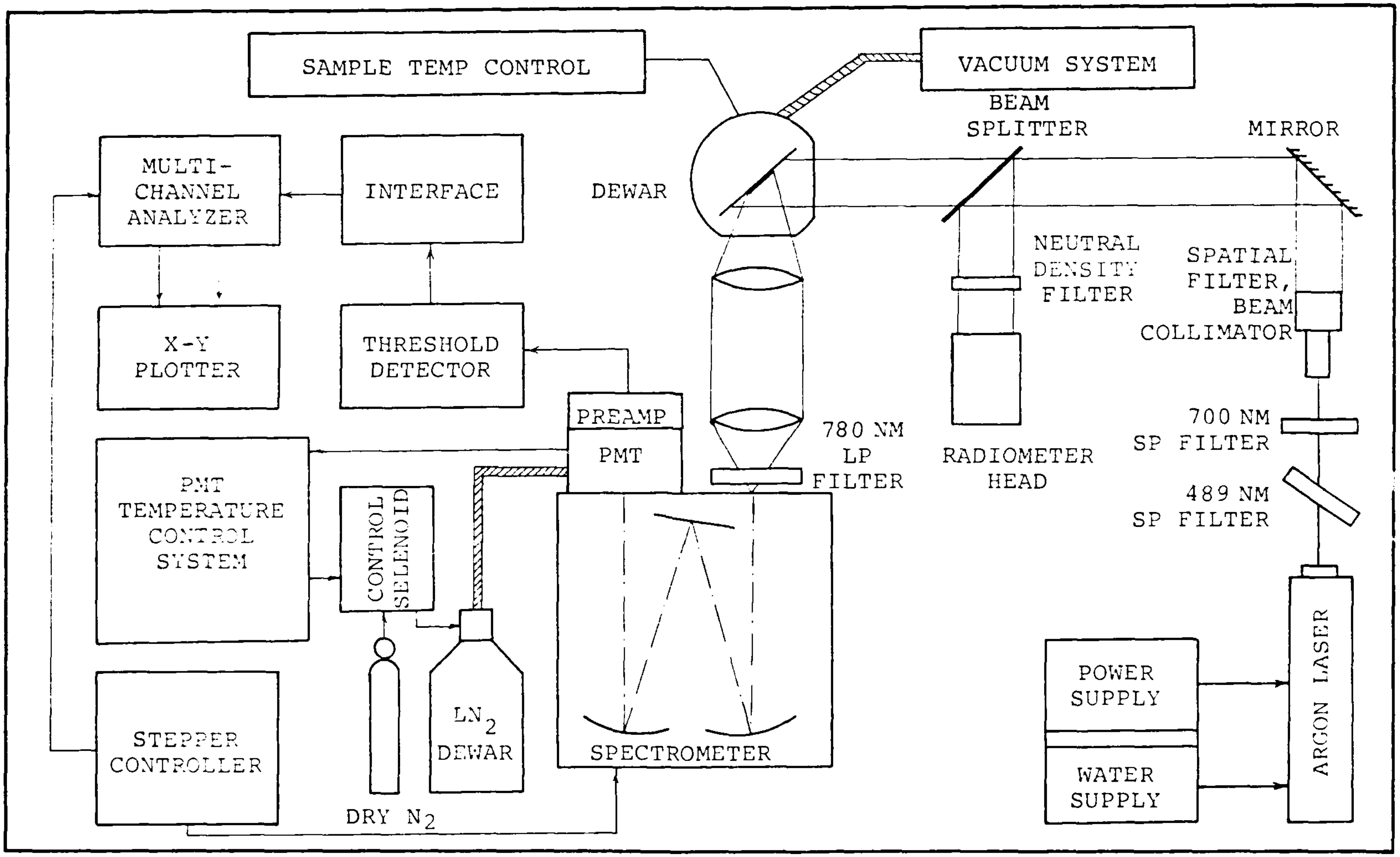

Fig. 4. Photoluminescence System Schematic

at the sample mount with a diameter of 16 mm was approximately four times as large as the exposed sample area. This was intentionally done to minimize the existence of power gradients across the sample caused by the inherent gaussian intensity profile of the laser beam. The quasi-lambertian nature of the portion of the beam profile to which the sample was exposed provided near-uniform illumination of the sample.

The photoluminescence emitted by the sample was collected by a bi-convex 76.2 mm lens placed one focal length away from the sample. The resultant parallel light was directed towards another bi-convex lens with a focal length of 200 mm which was placed one focal length from the entrance slit of the spectrometer. A 780 nm long pass filter was placed between the 200 mm lens and the spectrometer to eliminate any violet/ultraviolet radiation present as well as any specular reflections of the laser beam from the sample, which might have created higher order lines in the output spectrum.

The emitted sample PL was dispersed by a Czerny-Turner type 3/4 meter spectrometer (Spex, Model 1702). The grating used was 10 cm by 10 cm and contained 1200 grooves/mm blazed at 5000 Å. All the data was taken using slit widths of 0.5 mm. A slit height of 10 mm was used in all cases to insure that the sample image overfilled the entrance slit. Since the PL collection components required to match the f/number of the spectrometer were not available, it was necessary to use those previously described, which did, at least, overfill the grating. The spectrometer scan rate signal was externally provided by a locally assembled stepper/controller which yielded a scan rate of approximately 52 Å/minute.

Signal Detection and Processing

The output spectrum of the spectrometer was detected by a photomultiplier tube (PMT) (RCA, Model C70007A, with an S-1 type photocathode). The PMT was housed in a refrigeration chamber (Products for Research, Model TE-176-RF) which was mounted on the exit slit assembly of the spectrometer. A temperature controller (Products for Research) was used to maintain the PMT temperature at a constant -50°C by regulating the flow of LN to the PMT chamber. Prior to the collection of experimental data, a pulse height analysis experiment was conducted to determine the discrimination level and optimum signal-to-noise ratio of the PMT as a function of bias voltage and temperature. A bias voltage of 1350 V was used instead of the recommended 1250 V. This bias voltage was provided by a high voltage supply (Princeton Applied Research, Model HVS-1). The output of the PMT was connected to a threshold amplifier/discriminator (Princeton Applied Research, Model 1121) operated in a single threshold level mode. The output of the amplifier/discriminator was connected to an in-house-built interface which amplified, stretched and inverted the signal; properly conditioning it for processing by the multichannel analyzer (MCA) (Canberra, Model 8100/e). The frequency of the spectrometer stepper/controller was divided and used to trigger the MCA channel advance. The combination of the 52 Å/min drive rate and the frequency division resulted in an MCA resolution of 0.868 Å/channel. At the MCA, the threshold detected ulses were counted until the channel was advanced, then that number of counts was stored in a particular channel address. The process was continued until 1023 channels were covered. Then a plot of counts versus wavelength was displayed in the CRT display of the MCA in linear or logarithmic form. This plot was then transferred to an x-y plotter (Hewlett Packard, Model 7045A).

General Procedures

Prior to the introduction of LHe into the research dewar, the outer reservoir was filled with LN to precool the inner reservoir for approximately two hours. During the precooling, dry helium was introduced into the exchange column through the needle valve and capillary tube to continuously purge that area, and maintain a positive pressure to prevent the introduction of moist ambient air. Then, two samples were mounted, and the sample transfer rod was inserted and clamped into place. Reference marks on the sample transfer rod collar and exchange column collar were used to always place the samples at the same angle with the incident laser beam.

Once precooling was completed, the helium gas flow was stopped and liquid helium was introduced into the inner reservoir by means of an evacuated double-walled flexible tube connected to the LHe storage canister. Once full, the inner reservoir was sealed and allowed to self-pressurize by LHe vaporization. By adjusting the needle control valve, a sufficiently low amount of vaporizing LHe surrounded the sample which allowed it to be cooled, but which also allowed the relatively low power of the sample heaters to maintain the temperature set at the control panel. Throughout the experiment the temperature was set at 5°K. Sample cool-down was accomplished with the laser on so that any thermal effects from the laser could be taken into account, and to insure that the laser had reached a stable operating temperature and power level.

Once the optical components were aligned and the PL signal from the spectrometer was maximized, only small adjustments were necessary during the remainder of the experiment. Since the placement of the sample within the laser beam spot was critical, only two samples were mounted for each data run. The samples were mounted 2 mm apart, one above the other. This required only the vertical adjustment of the research dewar to properly place the particular sample of interest. Only one of the samples mounted in each run was used to gather data; the other was the same for all data runs of a particular type, and was used as a reference to check the repeatability of test conditions during each run. Although the repeated removal and replacement of the sample transfer rod resulted in a higher LHe consumption rate, this procedure provided the most consistently reproducible conditions.

Once the sample temperature reached a steady state, the laser output was readjusted and all switch positions were crosschecked. After reducing ambient light to a minimum, the spectrometer drive was begun. Shortly after this, an argon calibration lamp was uncovered near the entrance slit of the spectrometer to introduce two lines of known wavelength. The lines used were the 8006.16 Å line and the 8014.79 A line. Once these peaks were detected the argon lamp was covered. During the data run, which lasted either 17 minutes or 34 minutes, depending on the size of the spectrum being examined, the sample incident irradiance (nominally 20 mW/cm^2) and temperature were carefully monitored. After completion of the run, the plot on the CRT was examined and all data recorded prior to generating a hard copy on the x-y plotter. Throughout this thesis, the spectral plots were generated in logarithmic form because of the greater ease of scaling peaks of greatly differing magnitudes.

IV. Results of the Experiment

This chapter contains a description and analysis of the results of the experiment. But before these are discussed, sections are included which cover sample information and processing, as well as chemical etching procedures used.

Sample Information and Processing

The gallium arsenide samples (designated MR A001/R3) used in this effort were produced by the Materials Research Corporation. The samples were high-purity semi-insulating bulk material grown by the Liquid-Encapsulated Czochralski (LEC) method. A spark source mass spectrographic analysis of the material was conducted by Wright State University, Dayton, Ohio for AFWAL/AADR and reported by Dennis C. Walters on 16 October 1981. The results of that analysis are summarized in Table 2, and show that Si and C are the predominant impurities.

The two and one-half inch diameter wafers were cut into samples measuring 5 mm by 5 mm. The samples were then thoroughly cleaned in a vibration cleaner while sequentially submerged in beakers containing trichloroethylene (TCE), acetone, and methanol. This was followed by rinsing

TABLE 2

SPARK SOURCE MASS SPECTROGRAPHIC ANALYSIS OF GaAs SAMPLE (ppma)

Element	
Te	<.04
Se	<.02
Zn	<.04
Cu	<.03
Ni	<.05
Fe	<.03
Mn	<.02
Cr	<.02
S	<.05
Si	0.3
B	<.03
C	<0.1
AL	<.03
Mg	<.03

in deionized water and drying in a stream of dry nitrogen gas.

All the samples were then etched in a hot solution of $H_2SO_4:H_2O_2:H_2O$ in proportions of 3:1:1 for one minute. This was done in an effort to remove the layers of material that were damaged by the chemo-mechanical polishing by the manufacturer. The intent of this procedure was to remove approximately 15 microns from the surface. However, a subsequent experiment to determine the actual etch depth showed that this procedure removed only about 6 microns. Unfortunately, this was not discovered until after the samples had been completely prepared for the experiment, and a lack of time precluded the generation of a whole new set of samples.

After surface etching, the samples were again cleaned and then implanted with silicon at an energy of 120 KeV with dosages of 10^{12}, 10^{13}, 10^{14} and 10^{15} ions/cm^2. Figure 5 shows the expected ion concentrations for each of these four implant fluences as a function of sample depth as predicted by LSS theory. This data was provided by AFWAL/AADR. The unimplanted samples as well as those implanted at the four different dosages were then divided into three equal groups. Two of the groups were then capped using plasma deposited Si_3N_4 with a thickness of approximately 1200 Å. Each of the capped samples was then annealed for 15 minutes; one group at 750°C and the other at 900°C. Table 3 is a summary of sample designation and processing.

Chemical Etching Procedures

All sample layer removals were accomplished by using solutions of H_2O-H_2O_2-H_2SO_4 (Ref 18:769). For shallow layers of 150 Å, 250 Å, 500 Å, 1000 Å, a solution of 50 H_2O:1 H_2O_2:1 H_2SO_4 was used. By exposing the samples to a cold (ice bath) solution for 30 seconds and 60 seconds, etchings 150 Å deep and 250 Å deep respectively were achieved. By using the same solution at room temperature, for the same time periods stated above, etch depths of

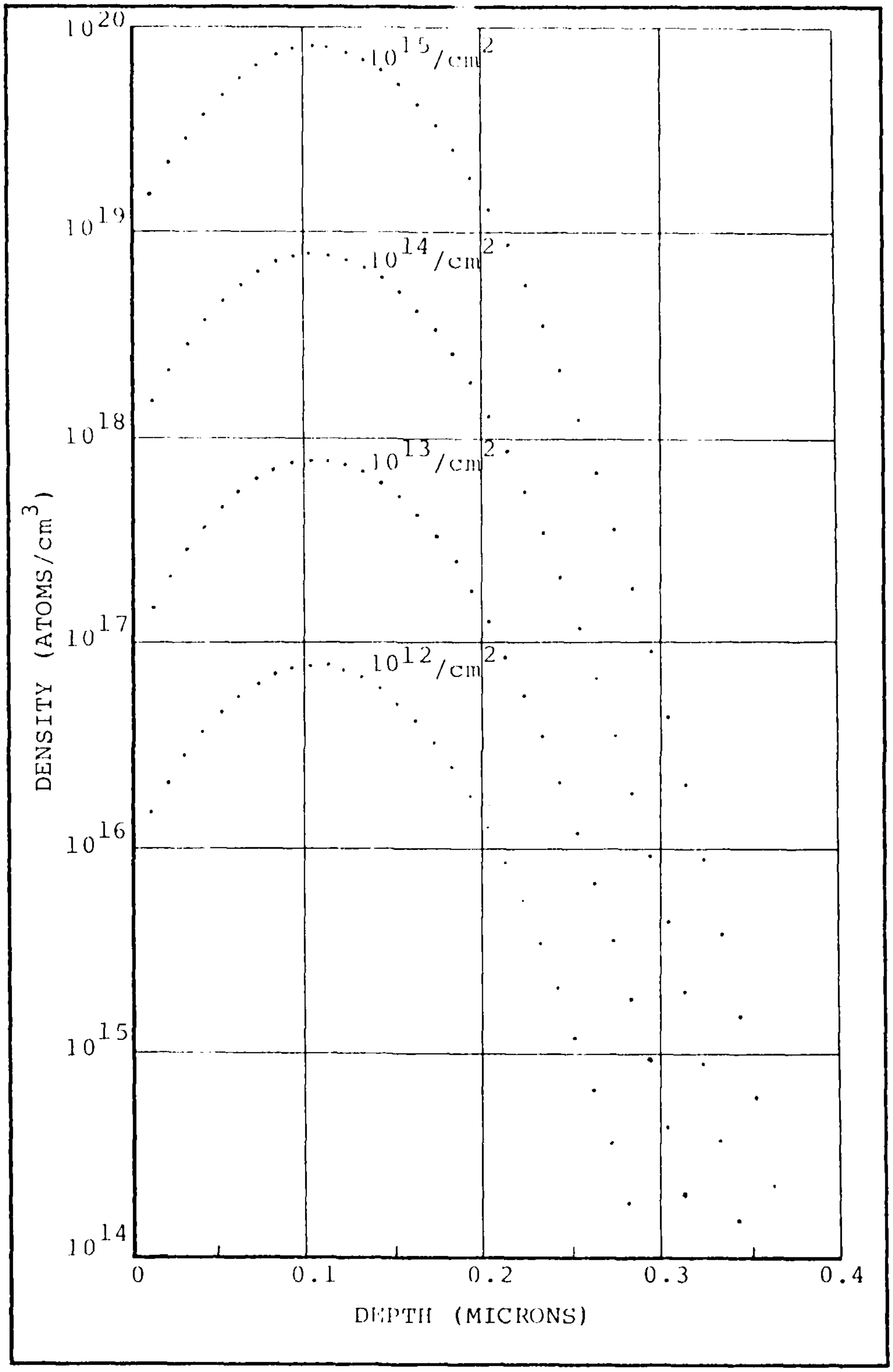

Fig. 5. Concentration of 120 KeV Si into GaAs

TABLE 3

SUMMARY OF SAMPLE DESIGNATION AND PREPARATION

Sample Designation	Implant Dosage	Annealing Temperature
1	None	None
2	None	750°C
3	None	900°C
4	$10^{12}/cm^2$	None
5	$10^{12}/cm^2$	750°C
6	$10^{12}/cm^2$	900°C
7	$10^{13}/cm^2$	None
8	$10^{13}/cm^2$	750°C
9	$10^{13}/cm^2$	900°C
10	$10^{14}/cm^2$	None
11	$10^{14}/cm^2$	750°C
12	$10^{14}/cm^2$	900°C
13	$10^{15}/cm^2$	None
14	$10^{15}/cm^2$	750°C
15	$10^{15}/cm^2$	900°C

500 Å and 1000 Å resulted. Deep etchings (1 micron) were achieved with a solution of 3 H_2SO_4:1 H_2O_2:1 H_2O. After the chemicals were mixed the sample was submerged while the solution was still hot from the reaction. This procedure yielded an etch rate of approximately 6 microns/minute. The actual etch rate was found to be extremely sensitive to the proportion of the chemicals, sample exposure time and temperature. Because of this, during the experiment, all etch depths were measured with a surface profile measuring instrument (Sloan Dektak) before etching conditions were changed. An etch reference sample was etched simultaneously with the PL data sample. Part of the etch reference sample was covered with wax to produce a reference surface. After a series of etchings at a particular rate were completed, the wax was removed, the etch depth was measured, and the average depth per etching was computed.

Experimental Results

As an initial step, the photoluminescence of all the generated samples was measured to determine the more likely candidates to be used for further investigation. Prior to this measurement the Si_3N_4 caps were removed from the annealed samples by submerging them in hydrofluoric acid for approximately five minutes.

PL of Unannealed Samples

Figures 12 through 16[1] show the spectra of the five unannealed samples. Figure 12 shows the PL of the virgin sample from approximately 1.55 eV to 1.36 eV. The weak peak at 1.513 eV is attributed to shallow donors (possibly Si). The previous assignment of this peak to free exciton transitions by some authors is believed to be in error (Ref 15:994). The weak nature of this line is characteristic of bulk-grown materials (Ref 19:1641). The broad peak near 1.490 is attributed to donor-acceptor pair recombination due to carbon donors (C_{Ga}) and carbon acceptors (C_{As}), and has been often observed by other researchers (Ref 20:36). It is apparent from Figure 12 that the broad peak near 1.4903 eV is actually a triplet of peaks; an accurate resolution of the other two peaks could not be obtained from this sample. Finally, the peak near 1.4543 eV, located 36 meV from the 1.4903 eV peak, is believed to be a phonon (1LO) replica of that peak. The absence of the conduction band-to-bound acceptor due to Si near 1.470 eV should be noted.

Figures 13 through 16 show the PL of samples implanted with the successively increasing dosages, and demonstrate the reduction of PL efficiency caused by implantation damage even at low (10^{12} ion/cm^2) dosages. Samples number 1, 7, 10, and 13 were chosen for further investigation.

---

[1] Figures numbered 12 through 26 appear in the appendix.

PL of Samples Annealed at 750°C

Figures 17 through 21 show the PL of the samples annealed at 750°C for 15 minutes. The photoluminescence efficiencies of the 1.513 eV and 1.490 eV peak increased by a factor of 7.5 and 4.6 respectively over those of the unannealed virgin sample. The energies of all the peaks as well as the transitions believed to be responsible for their presence are listed in Table 4.

TABLE 4

SAMPLE 2 SPECTRAL LINES

Line No.	Energy (eV)	
1	1.5162	Exciton Transition (Ref 11:342)
2	1.5130	Shallow Donor
3	1.4901	C Donor to C Acceptor (Ref 20:36)
4	1.4870	Donor to Z_N Acceptor (Ref 20:37)
5	1.4537	Phonon Replica of #3
6	1.4503	Phonon Replica of #4
7	1.4059	As Vacancy Complex to Si Acceptor (Ref 21:1097)
8	1.3581	Ga Vacancy Complex
9	1.3223	Phonon Replica of #8

Figures 18 through 21 show the effects of the different dosages on the PL spectra. The broadening and increasing intensity of the lower energy peaks associated with vacancy complexes was also present in the samples annealed at 900°C. An attempt to better characterize this phenomena is made shortly in this chapter.

PL of Samples Annealed at 900°C

The PL spectra of the samples annealed at 900°C had much the same characteristics as those annealed at 750°C. Figure 22 shows the PL of the virgin sample. The 1.513 eV peak and the 1.490 peak increased in intensity by factors of 68 and 34 respectively over those of the unannealed samples. Although the mechanisms behind this are not yet fully understood, it is believed that the short-time heat treatment of melt-grown GaAs improves radiative efficiencies through the elimination of both deep acceptor traps and nonradiative defect centers, as well as an increase of shallow donor concentrations with increasing anneal temperature (Ref 19:1642, 1644).

PL of Sample 15

Sample 15, which was implanted with a dosage of 10^{15} ions/cm^2 and then annealed at 900°C for 15 minutes, was further investigated to determine its usefulness in the study of ion implantation damage as well as to study the nature of the low energy broad band peaks. The PL of the sample was taken at four different temperatures. The resulting spectra are shown in Figure 6. At 77°K (Figure 6(a)), the dominant peak was centered at approximately 1.384 eV. As the temperature was decreased to 30°K (Figure 6(b)), the intensity of the 1.38 eV peak increased, and a new broad peak centered at about 1.423 eV appeared. With further reductions in temperature to 15°K and 5°K (Figures

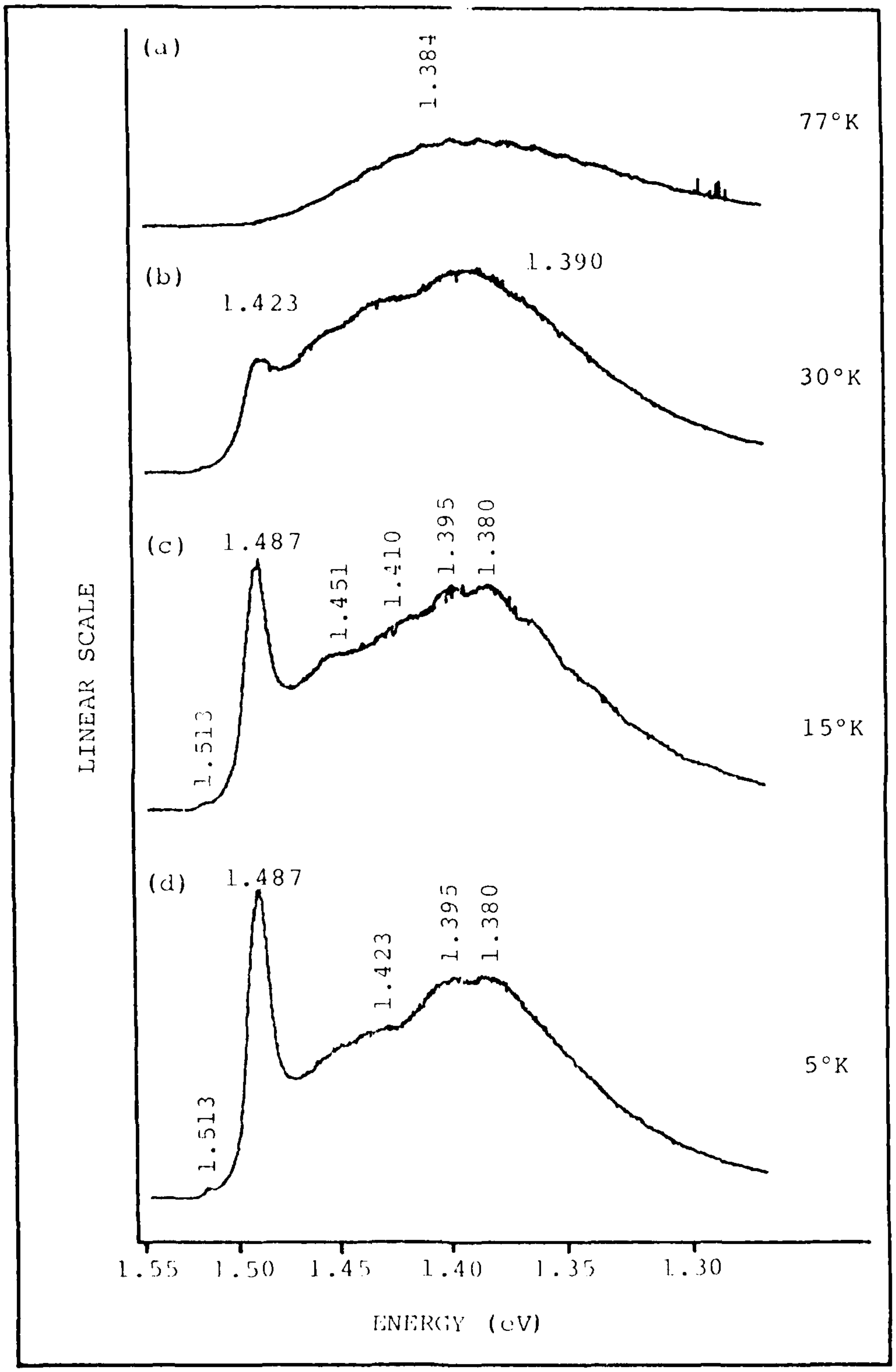

Fig. 6. PL of Sample #15 with Variations in Temperature from 5°K to 77°K

6(c) and 6(d)), these two peaks continued to increase in intensity but remained approximately constant relative to each other. No significant change in peak position was observed due to the temperature change; however, no conclusions could be made on the temperature dependence of these transitions over the small temperature range tested.

The next step was to etch the sample chemically, and observe the behavior of the peaks at 5°K. Figure 7 shows the resulting PL spectra. The principal change noticed between Figures 7(a) and 7(b) is that the dominant peak at about 1.38 eV at the surface was overshadowed by the peak at about 1.42 eV at a depth of 500 Å. The magnitude of the 1.42 eV line increased by a factor of nearly 2 at 500 Å, and at 1000 Å, by a factor of nearly 4. This suggests, considering Figure 5, that the amplitude of these peaks is highly dependent on the Si concentration. Figures 7(d) and 7(e) show that at a depth of 2000 Å the 1.38 eV and 1.42 eV peaks had been greatly reduced and that at ~10,000 Å the PL spectra had returned to that of the virgin sample. The nature of the low energy broad transitions is believed to involve deep level complexes associated with Si in As sites and As vacancies (Ref 22:6188). These transitions are also thought to be complicated by the presence of multiple Si acceptor states as well as deep band tail states below the conduction band created by the high Si concentration (Ref 23:2009). In analyzing the surface PL of samples annealed at 750°C and 900°C, it was

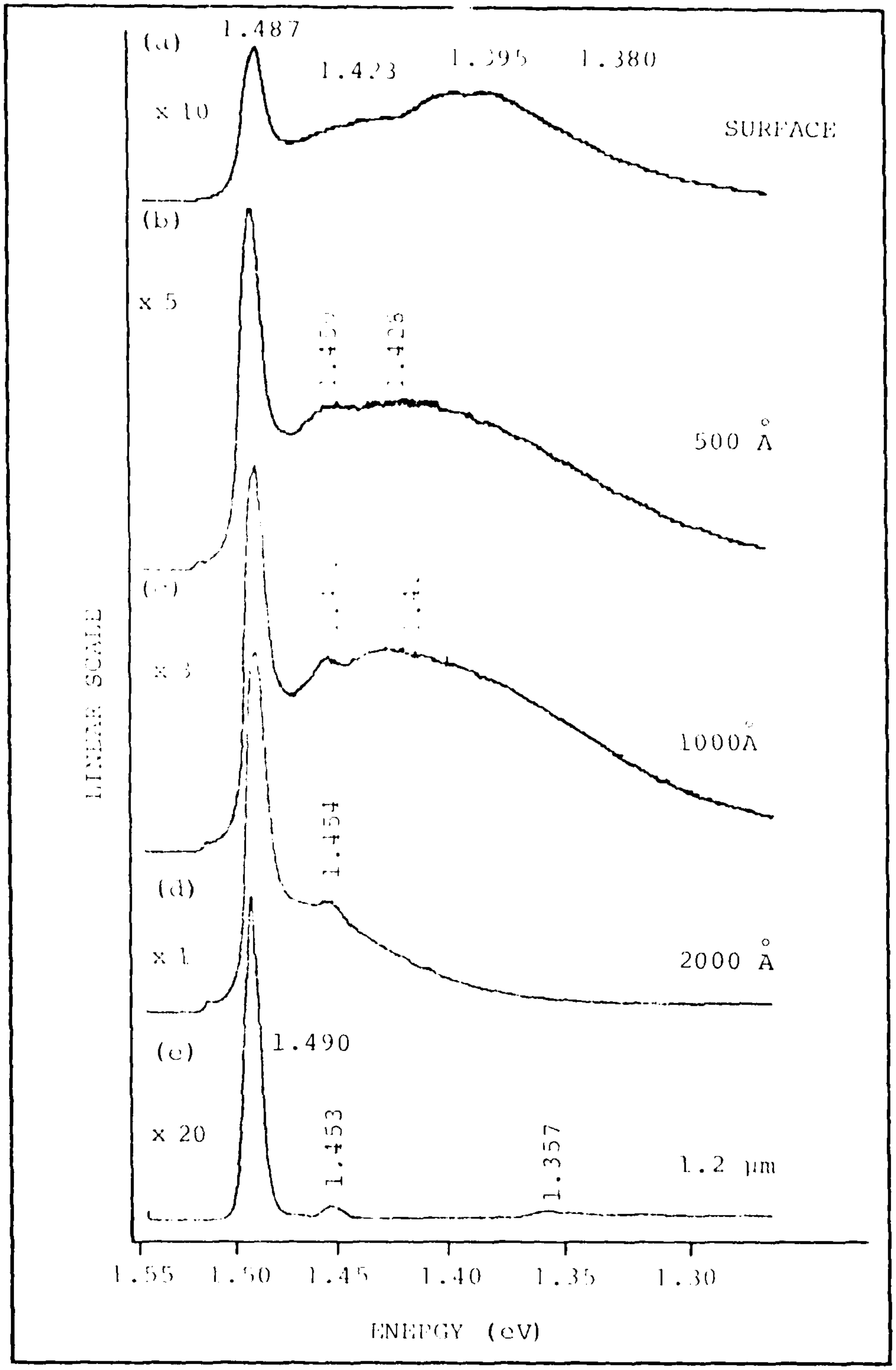

Fig. 7. PL of Sample #15 as Surface Layers were Removed

noticed that as the implant dosage increased, very little change occurred in the intensities of the peaks near 1.513 eV and 1.490 eV. The greatest increase was seen in the low energy peaks mentioned above. This suggests that the majority of the implanted silicon was activated into vacancy complexes involving arsenic vacancies, which form mostly within a micron of the surface (Ref 24:229). Further characterization of the broad low energy bands would require further detailed experimentation which, because of time constraints, is not within the scope of this thesis.

Because of the uncertainty and complexity of the radiative mechanisms in the annealed samples, as well as the healing effects of annealing; it was decided that only the unannealed samples would be used to study damage due to ion implantation.

Depth Distribution of Defects in Unannealed Samples

The samples chosen were those implanted with dosages of 10^{13}, 10^{14}, and 10^{15} ions/cm^2 (samples 7, 10, and 13). In order to get the depth distribution of defects, the photoluminescence at 5°K was measured by successive etching of the sample surfaces. Prior to etching the implanted samples, the homogeneity of PL was tested in a virgin sample using the procedure described above. The PL measurements were taken to a depth of approximately 30 microns; the intensities of which were found to remain within 10 percent of each other.

The surface PL measurements taken of all the unannealed samples (Figures 12 through 16) showed that the implantation damage did not cause any new radiative transitions in the material within the observed spectral range. The only effect was the successively increasing quenching of luminescence intensity with increasing dosage. As mentioned in Chapter II, the LSS theoretical prediction of the ion projected range is 1025 Å with a standard deviation of 510 Å. The theoretical damage profile is slightly shallower, and is depicted in Figure 8. This data, derived from a Monte Carlo simulation, was also provided by AFWAL/AADR. Figure 9, 10, and 11 show the change in intensity of the 1.490 eV peak as a function of depth for the three implant dosages. The PL intensity was normalized by that of a virgin sample which had been etched to approximately 25 microns below the original surface. The PL of both samples was measured in each run using the procedures described in Chapter III. The penetration depth or "skin depth" of the 488.0 nm laser light used was calculated to be 1050 Å, using a value of the imaginary part of the index of refraction at 21°K (Ref 25:522). The position and amplitude of the theoretical damage profile could not be resolved or accurately verified very neatly. This was due to the fact that the changes in PL intensity observed were a result of a convolution of the gaussian-like theoretical damage profile and the exponentially decaying illumination, which at the outset covered the majority of

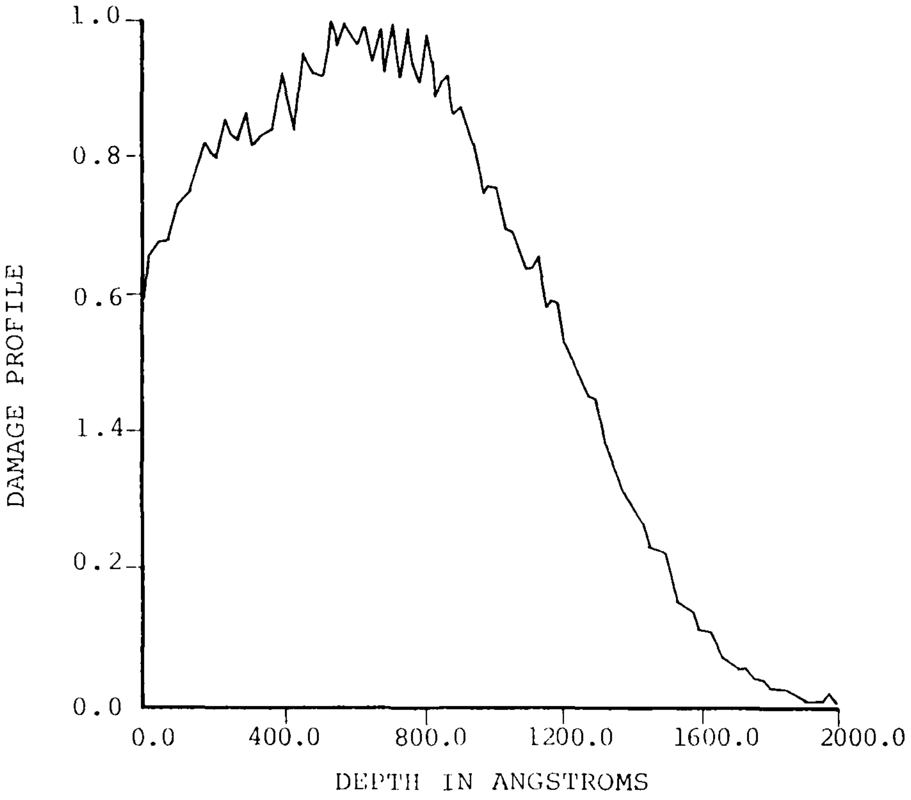

Fig. 8. Theoretical Damage Profile of
120 KeV Si into GaAs

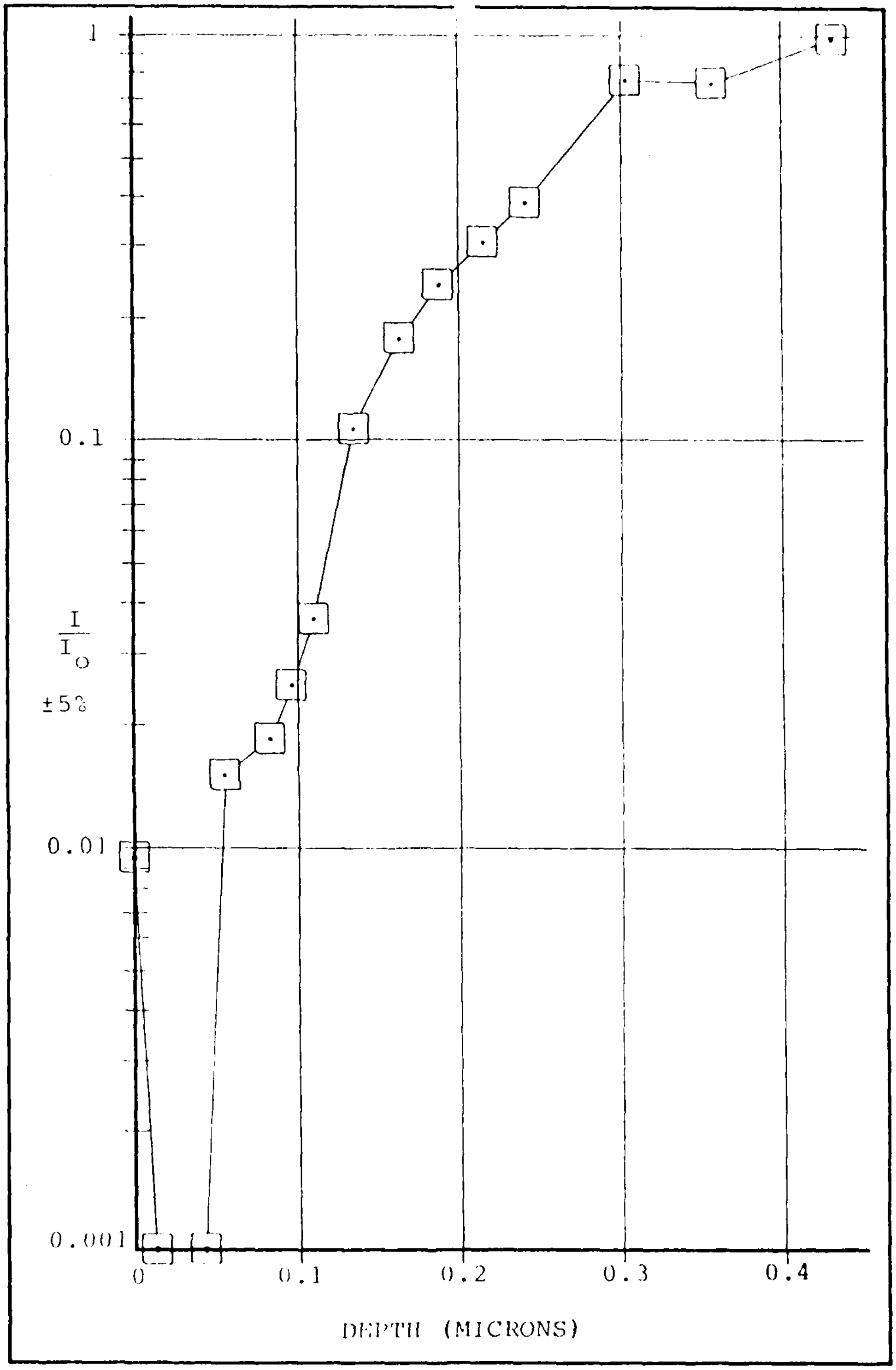

Fig. 9. Normalized PL of Sample Implanted with 10^{13} ions/cm^2 as Function of Depth

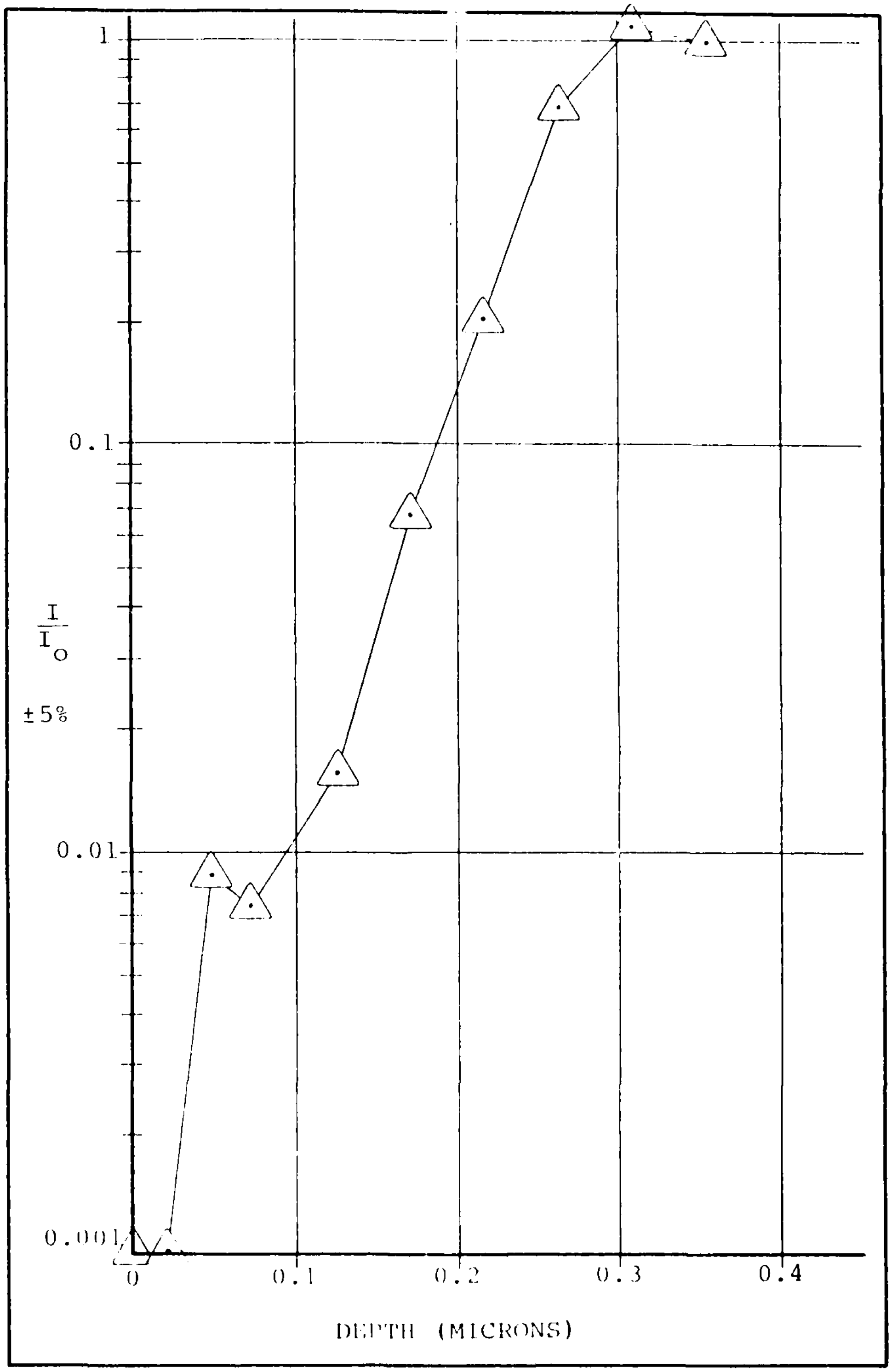

Fig. 10. Normalized PL of Sample Implanted with 10^{14} ions/cm^2 as a Function of Depth

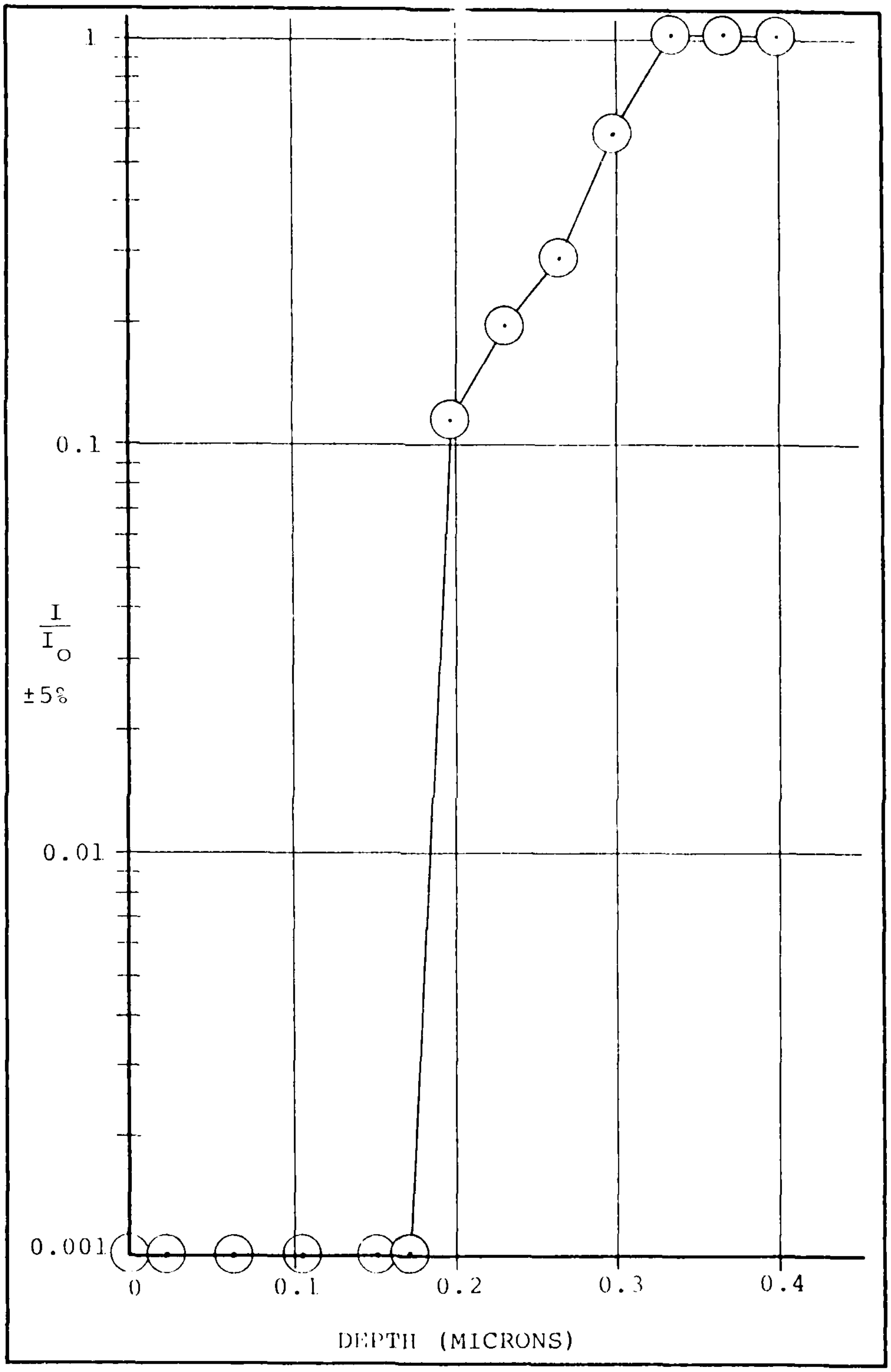

Fig. 11. Normalized PL of Sample Implanted with 10^{15} ions/cm^2 as a Function of Depth

the damage region. However, the behavior of the curves in Figures 9 and 10 within the first 1000 Å, give a hint of the presence of the predicted damage area. In the case of the 10^{15} ion/cm^2 implanted sample, the luminescence was totally quenched to a depth of approximately 1750 Å. The failure of the sample PL to be restored to that of the virgin material until depths of 4200 Å, 3000 Å, and 3300 Å, in the 10^{13}, 10^{14}, and 10^{15} ion/cm^2 implanted samples respectively, showed that the damage region extended deeper into the sample than predicted. Since the samples were implanted at room temperature, the likely cause is the diffusion of defects into the material. This is in qualitative agreement with previous work (Ref 7:405) except that the results of this study showed that defects did not diffuse as deeply in the case of silicon implants.

V. Conclusions and Recommendations

Conclusions

The implantation of silicon into the LEC grown semi-insulating GaAs samples did not generate damage peaks within the observed spectral range (1.55 eV to 1.27 eV), in the unannealed samples. The only effect observed was the increasing quenching of the native peaks with increasing dosage. The defects in these samples due to ion implantation were found to exist at a depth nearly twice that predicted by theory. This was attributed to the diffusion of defects during the room temperature implantation process. The fact that the sample luminescence returned to the virgin state suggests that the effects of surface chemo-mechanical polishing, which created some concern early in the experiment, proved not to be a significant factor at sample depths of approximately six microns.

Examination of the PL spectra of the annealed samples suggested that, since no peaks associated with simple silicon centers appeared, the majority of the silicon implanted became associated with arsenic vacancy complexes which formed low energy peaks near 1.38 eV and 1.42 eV. The intensity of these peaks was found to vary inversely with temperature, whereas the peak positions were not seen to vary in the range of 5°K to 77°K. These peak positions were found to vary as sample layers were removed. The material PL was found to return to that of the virgin material at approximately 1 micron of depth. This suggested a peak dependence in silicon concentration. The peaks were tentatively attributed to arsenic vacancy complexes associated with silicon. The use of the annealed samples for the study of ion implantation damage was abandoned due to the uncertain characterization and origin of the low energy peaks, as well as the damage healing effects of the thermal treatment.

Recommendations

It is recommended that detailed experimentation and analysis be performed on the samples annealed at 750°C and 900°C to determine the characteristics of the low energy broad peaks as well as the places and roles occupied by the implanted silicon atoms in the radiative and non-radiative processes of the material. These studies should include the dependence of the low energy peaks on changes in broad ranges of temperature, implant dosage, illumination intensity, and anneal temperature.

It is also recommended that, if future studies are to be made of the nature of ion implantation damage, either an ion species with a projected range greater than the skin depth of the 488.0 nm laser line be chosen, or another suitable source with a shorter skin depth be used. A more suitable experimental technique would involve the use of cathodoluminescence equipment and procedures. Additionally, the use of detectors sensitive in the range of 1.1 microns to 1.3 microns is recommended to explore that region of the spectrum.

Recommended improvements in the photoluminescence equipment setup used for this effort include the installation of a rigid support for the laser to preclude subjecting its cavity to bending and torsion moments. The present setup uses a 3/4 inch thick piece of plywood supported by two laboratory jacks. The wood was found to be sensitive enough to ambient temperature and humidity changes to cause power fluctuation in the laser due to changes in the resonant cavity parameters.

Bibliography

1. Air Force Avionics Laboratory, *Technical Programs and Contracts*, March 1979, 10th ed.

2. Pomrenke, Gernot S. *Photoluminescence of Undoped, Semi-Insulating, and Mg-Implanted Indium Phosphide*. MS thesis. Wright-Patterson AFB, Ohio: School of Engineering, Air Force Institute of Technology, December 1979.

3. Gershenzon, M. "Radiative Recombination in the III-V Compounds," *Semiconductors and Semimetals*, *Volume 2*, edited by R. K. Willardson and Albert C. Beer. New York: Academic Press, 1966.

4. Morgan, D. V. "The Characterization and Application of Ion-Induced Damage in Gallium Arsenide Devices," *Radiation Physics and Chemistry*, *15*:627-636 (March 1980).

5. Gavrilov, A., *et al*. "Photoluminescence Investigation of the Distribution of Defects in Gallium Arsenide After Ion Bombardment," *Soviet Physics of Semiconductors*, *10*(8):847-8 (August 1976).

6. Norris, C. B. and C. E. Barnes. "Cathodoluminescence Studies of Anomalous Ion Implantation Defect Introduction in Lightly and Heavily Doped Liquid Phase Epataxial GaAs: Sn," *Journal of Applied Physics*, *51*(11):5764-5772 (November 1980).

7. Aoki, K., et al. "Depth Distribution of Defects in Mg-Ion and Cd-Ion Implanted GaAs," *Japan Journal of Applied Physics*, *15*(2):405-6 (February 1976).

8. McKelvey, John P. *Solid State and Semiconductor Physics*. New York: Harper and Row, 1966.

9. Kittel, C. *Introduction to Solid State Physics*. New York: John Wiley and Sons, 1974.

10. Pankove, Jacques I. *Optical Processes in Semiconductors*. Englewood Cliffs, NJ: Prentice-Hall, Inc., 1971.

11. Williams, E. W., *et al.* "Photoluminescence II: Gallium Arsenide," *Semiconductors and Semimetals, Volume 8*, edited by R. K. Willardson and Albert C. Beer. New York: Academic Press, 1972.

12. Bebb, H. B., *et al.* "Photoluminescence I: Theory," *Semiconductors and Semimetals, Volume 8*, edited by R. W. Willardson and Albert C. Beer. New York: Academic Press, 1972.

13. Pankove, J. I. "Electroluminescence," *Topics in Applied Physics, Volume 17*, edited by Jacques I. Pankove. Berlin: Springer-Verlag, 1977.

14. Ashen, D. J., *et al.* "The Incorporation and Characterization of Acceptors in Epitaxial GaAs," *Journal of Physics and Chemistry of Solids*, *36*:1041-1053 (1975).

15. Bogardus, E. H. and H. B. Bebb. "Bound-Exciton, Free-to-Bound, Band-Acceptor, Donor-Acceptor, and Auger Recombination in GaAs," *Physical Review*, *176*:993-1002 (December 1968).

16. Lindhard, J., *et al.* "Range Concepts and Heavy Ion Ranges," *Mat. Fys. Medd. Dan. Vid.* Selsk *33*:1 (1963).

17. Gibbons, James F. *Projected Range Statistics*. Stroudsburg, Pa.: Dowden, Hutchinson and Rose, Inc. (1975).

18. Iida, S., *et al.* "Selective Etching of Gallium Arsenide Crystals in H_2SO_4-H_2O_2-H_2O System," *Journal of the Electrochemical Society: Solid State Science*, *118*(5): 768-771 (1970).

19. Kushiro, Y., *et al.* "Improved Properties of Melt-Grown GaAs by Short-Time Heat Treatment," *Journal of Applied Physics*, *46*(4):1636-1645 (April 1977).

20. Parzianello, L. V. *Depth-Resolved Cathodoluminescence of Carbon Implanted Gallium Arsenide*. MS thesis. Wright-Patterson AFB, Ohio: School of Engineering, Air Force Institute of Technology, December 1978.

21. Yu, P. W. and Y. S. Park. "Photoluminescence in Mn-implanted GaAs--an Explanation of the 1.40 eV Emission," *Journal of Applied Physics*, *50*(2):1097-1103 (February 1979).

22. Lum, W. Y. and H. H. Weider. "Photoluminescence of Thermally Treated n-type Si-doped GaAs," *Journal of Applied Physics*, *49*(12):6187-88 (December 1978).

23. Kressel, H., et al. "Luminescence in Silicon-Doped GaAs Grown by Liquid-Phase Epitaxy," Journal of Applied Physics, 39(4):2006-2011 (March 1968).

24. Itoh, T. and M. Takeuchi. "Arsenic Vacancy Formation in GaAs Annealed in Hydrogen Gas Flow," Japanese Journal of Applied Physics, 16(2):227-232 (February 1977).

25. Seraphin, B. O. and H. E. Bennett. "Optical Constants," Semiconductor and Semimetals, Volume 3, edited by R. K. Willardson and Albert C. Beer. New York: Academic Press, 1967.

Appendix

Photoluminescence Spectra of Samples Prior to Etching

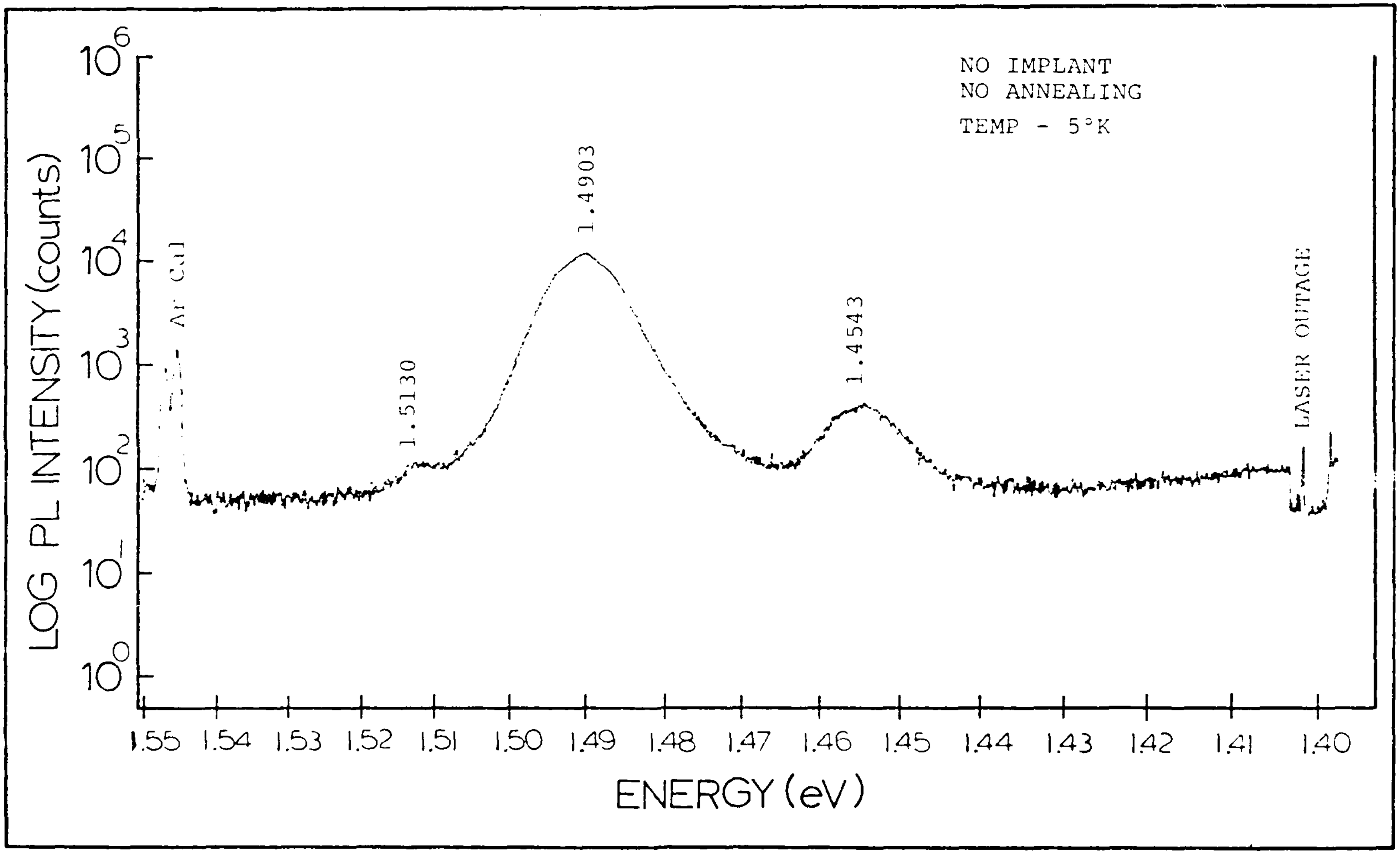

Fig. 12. PL of Sample 1

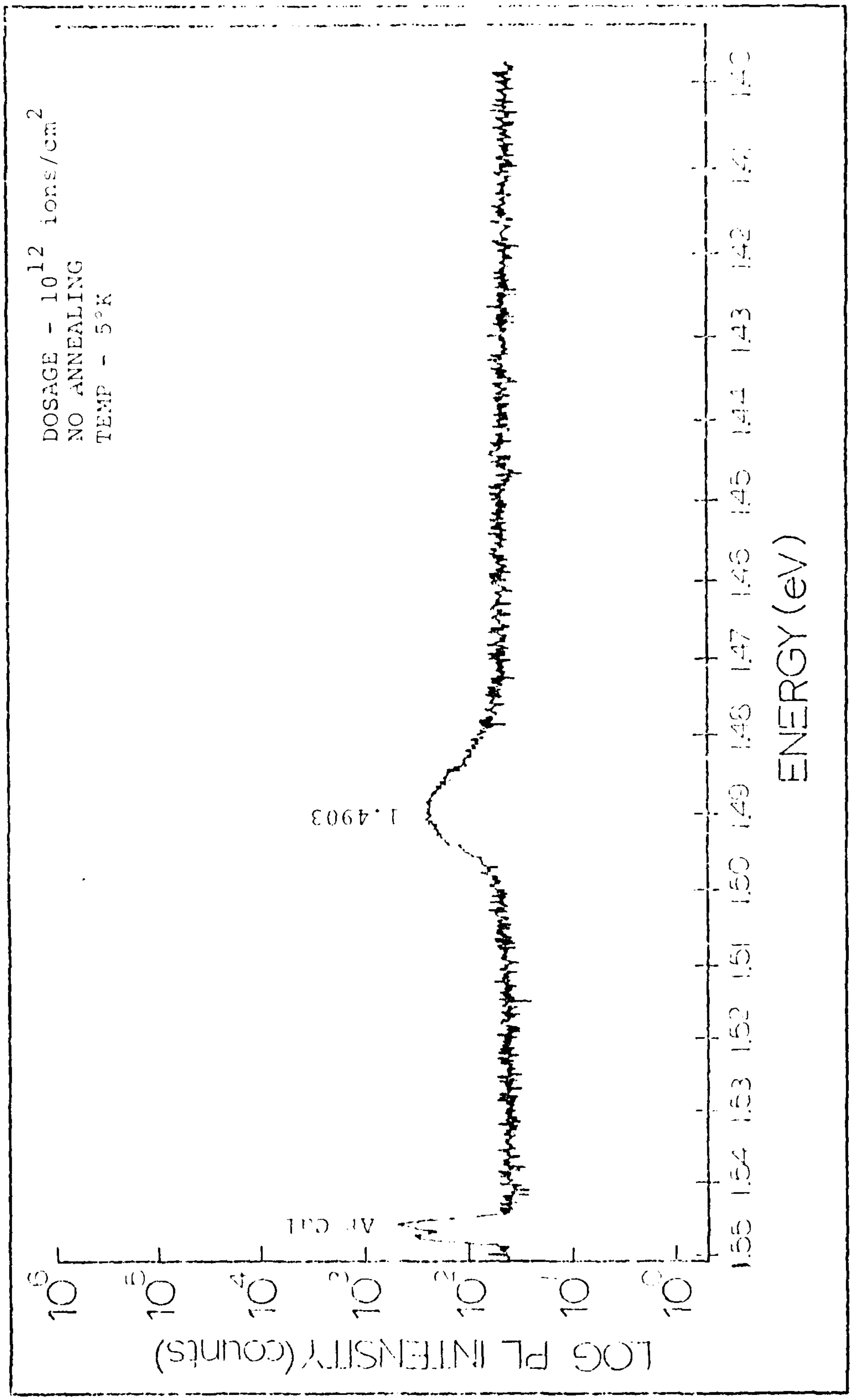

Fig. 13. PL of Sample 4

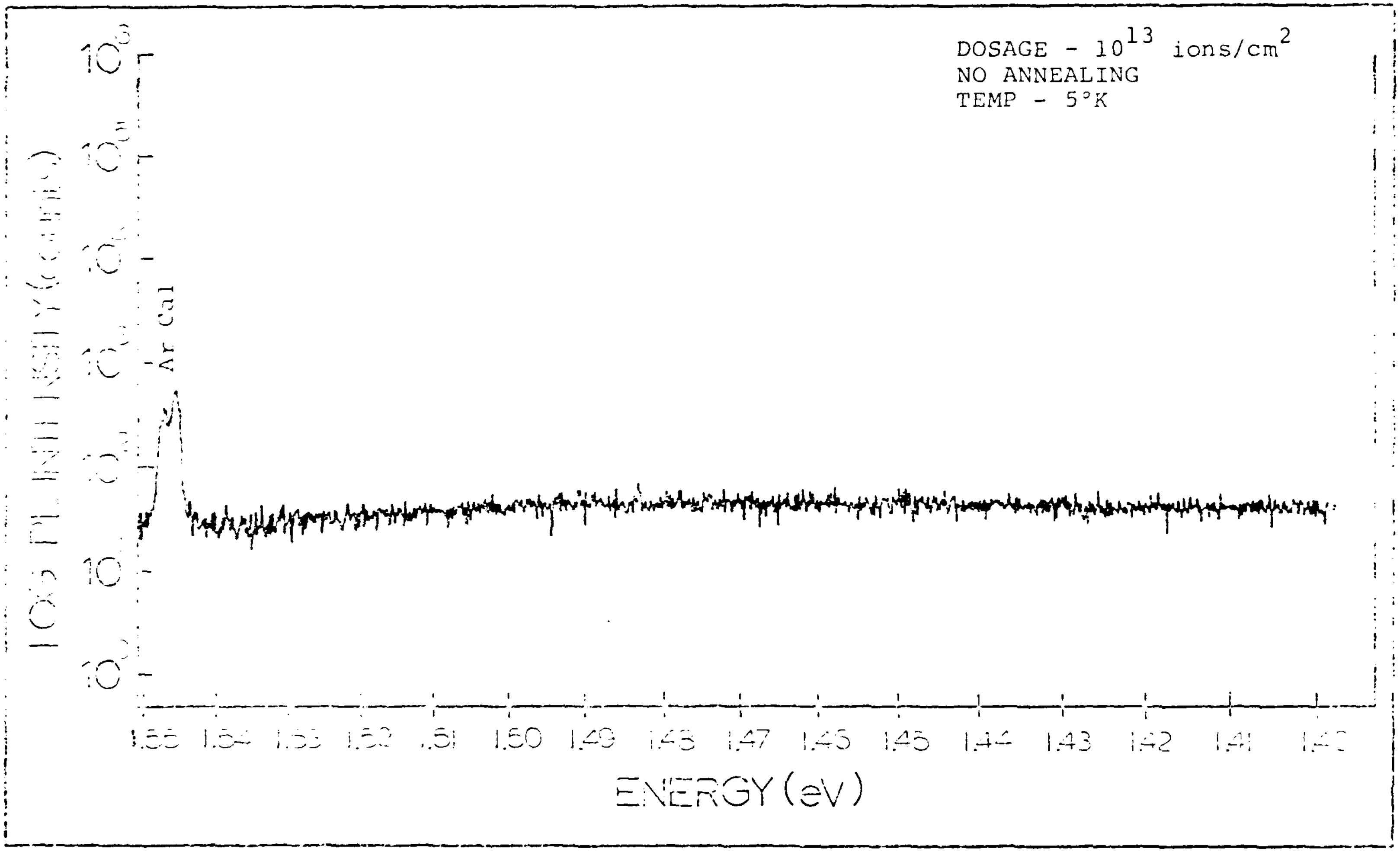

Fig. 14. PL of Sample 7

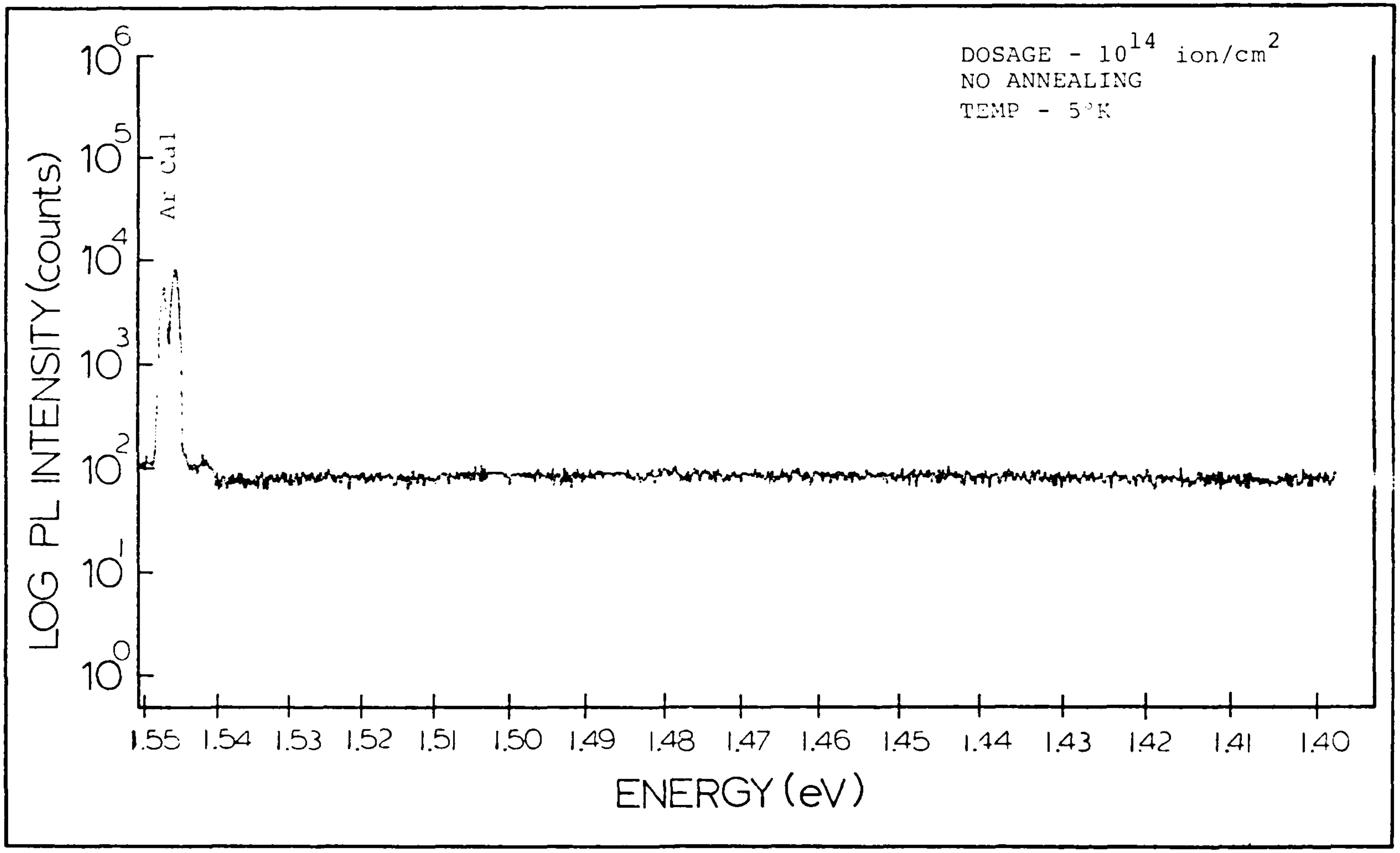

Fig. 15. PL of Sample 10

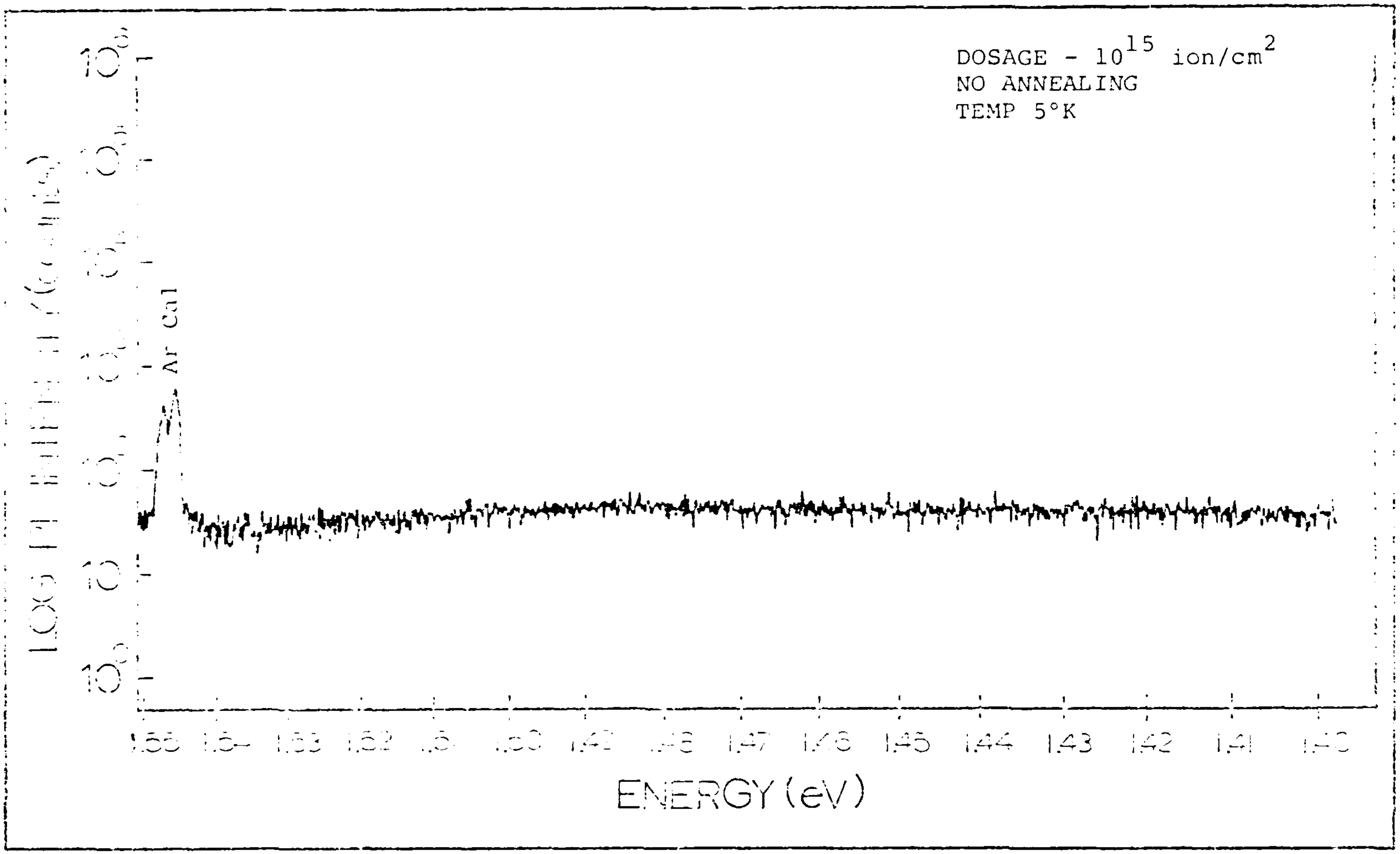

Fig. 16. PL of Sample 13

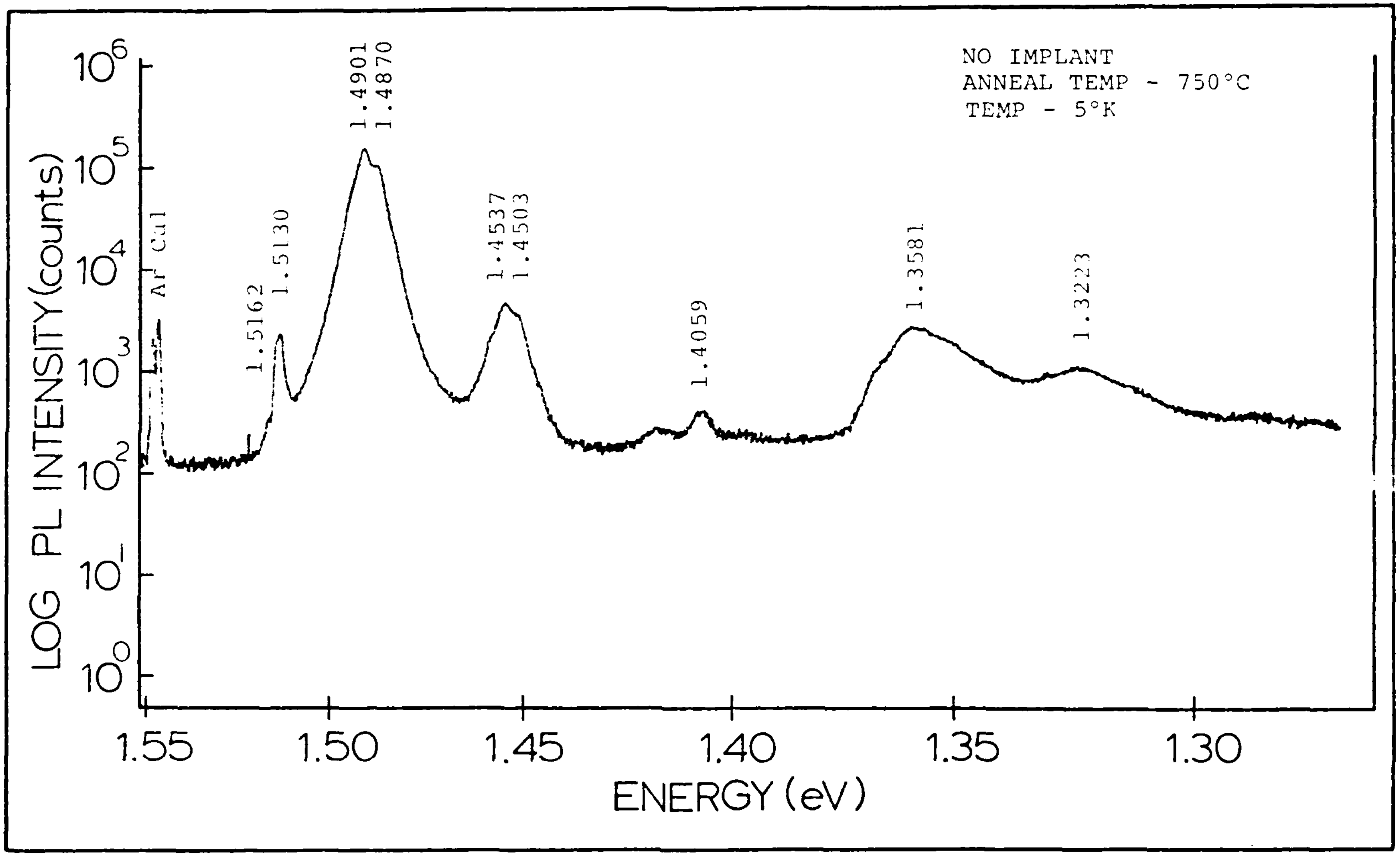

Fig. 17. PL of Sample 2

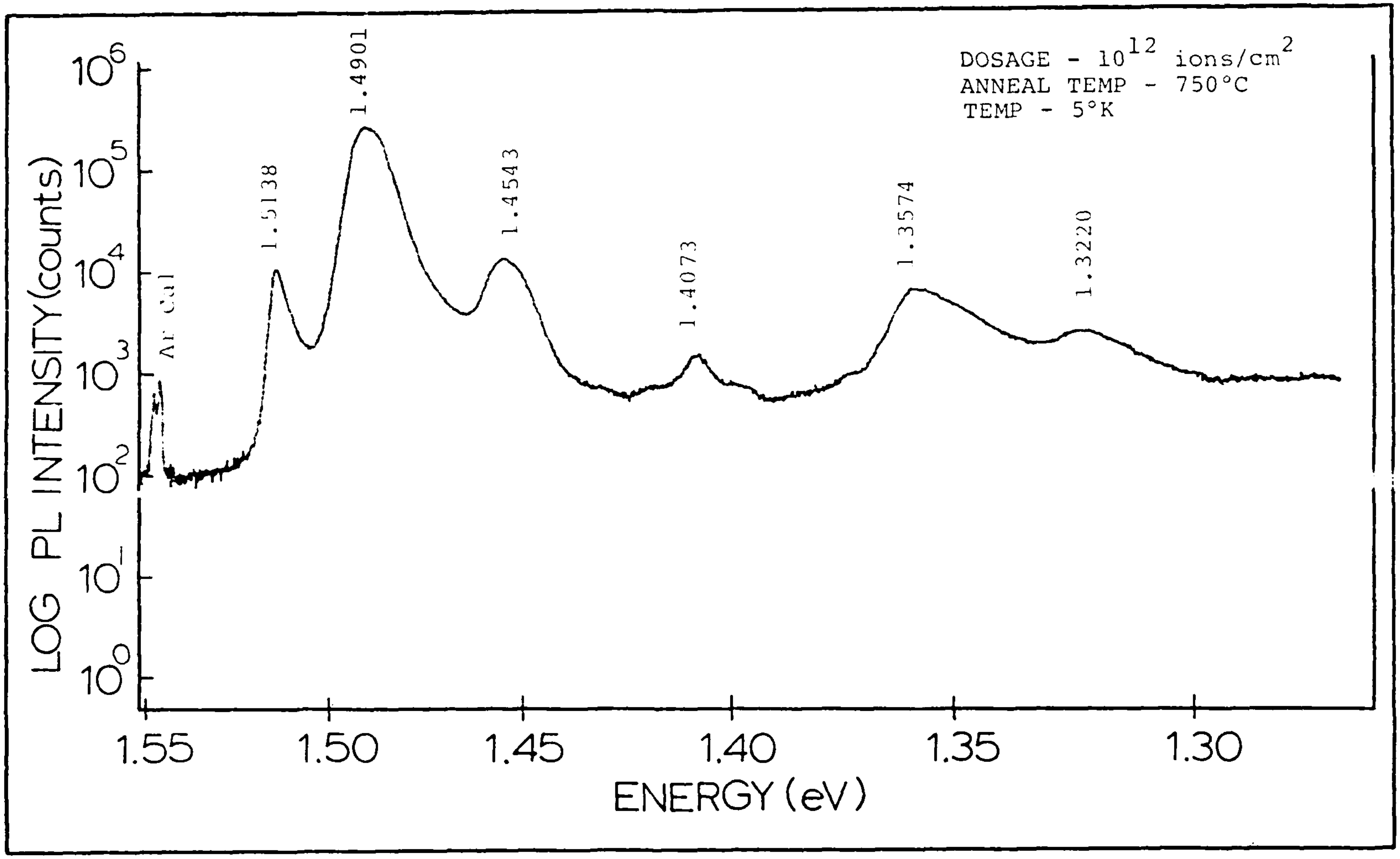

Fig. 18. PL of Sample 5

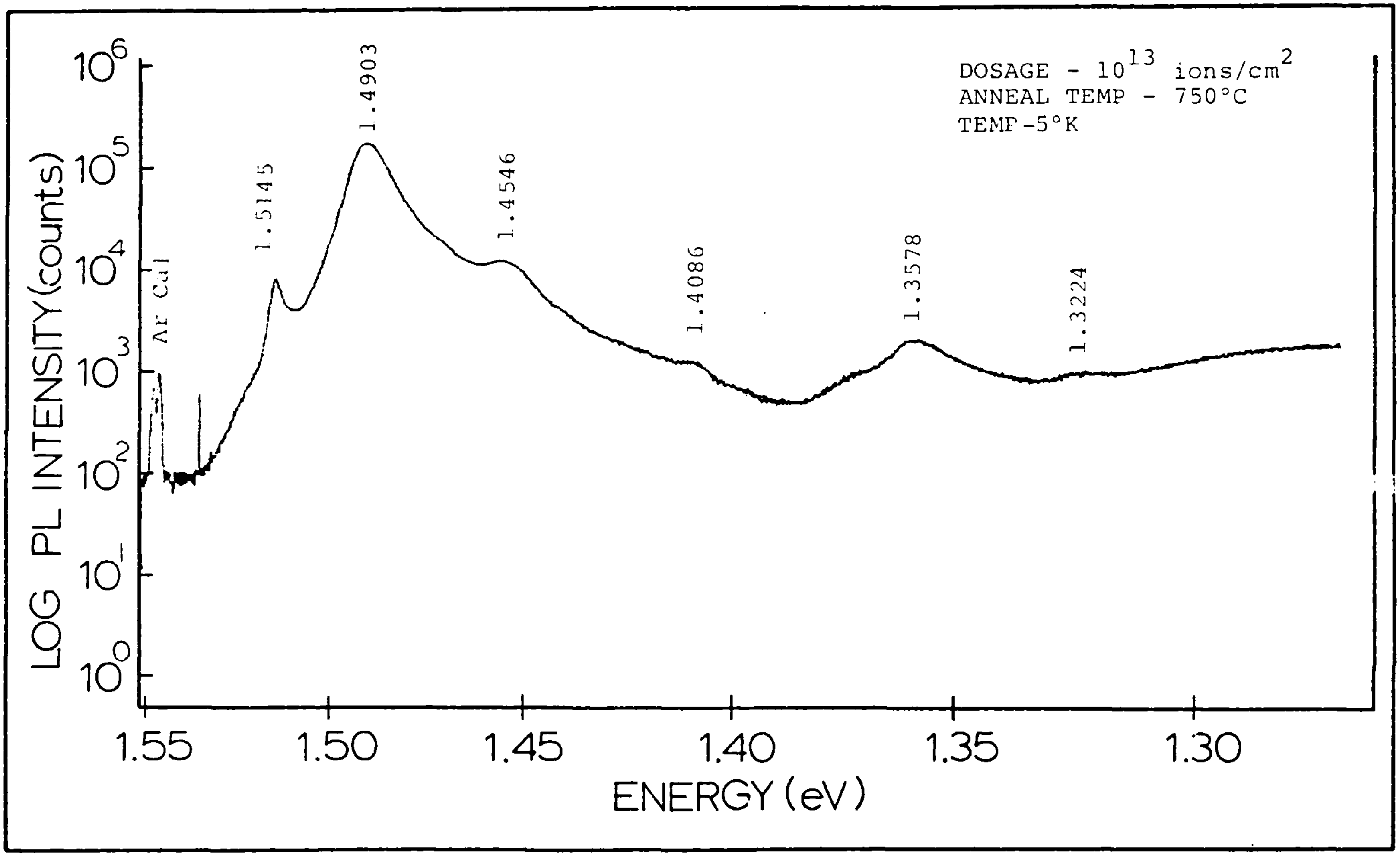

Fig. 19. PL of Sample 8

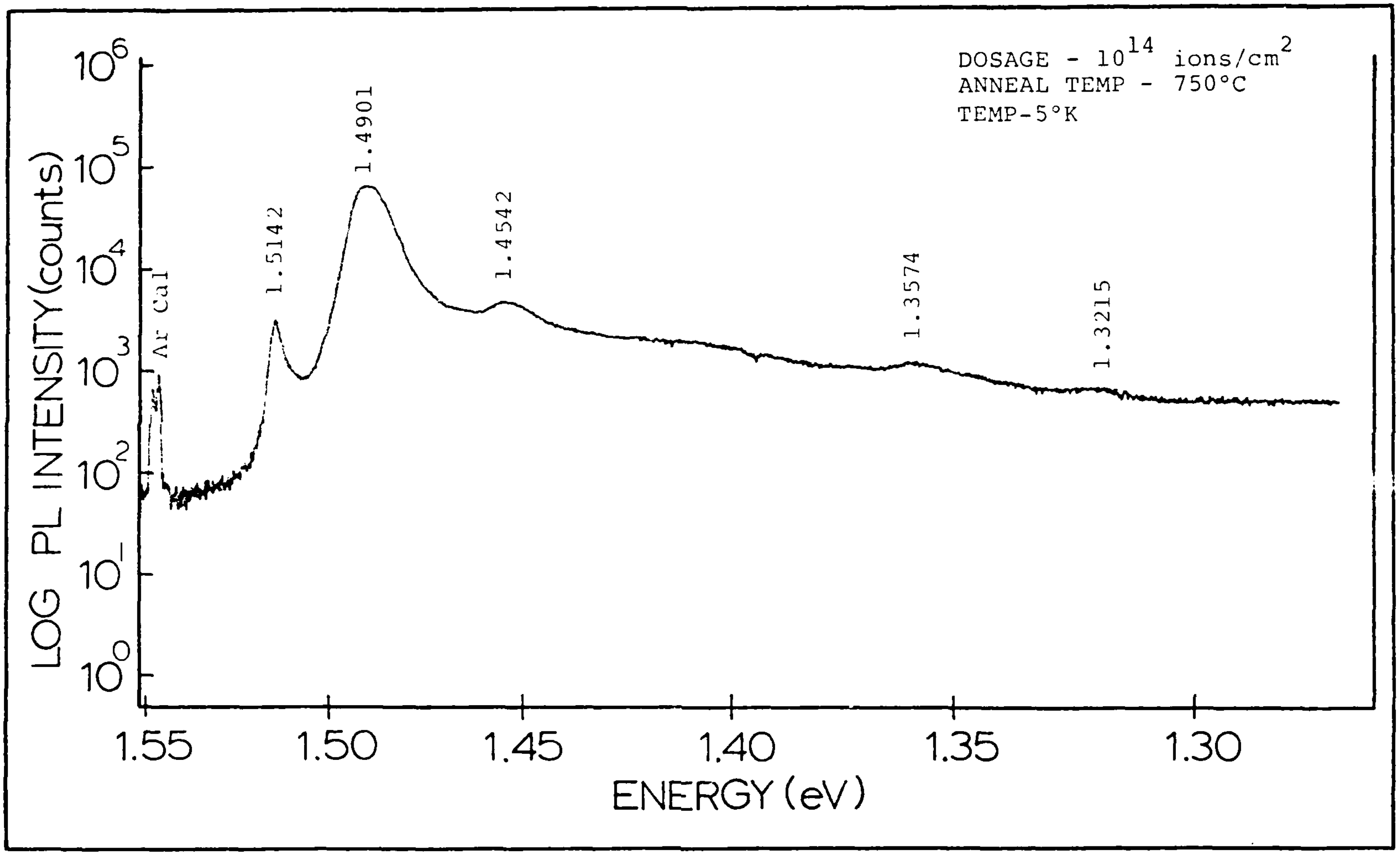

Fig. 20. PL of Sample 11

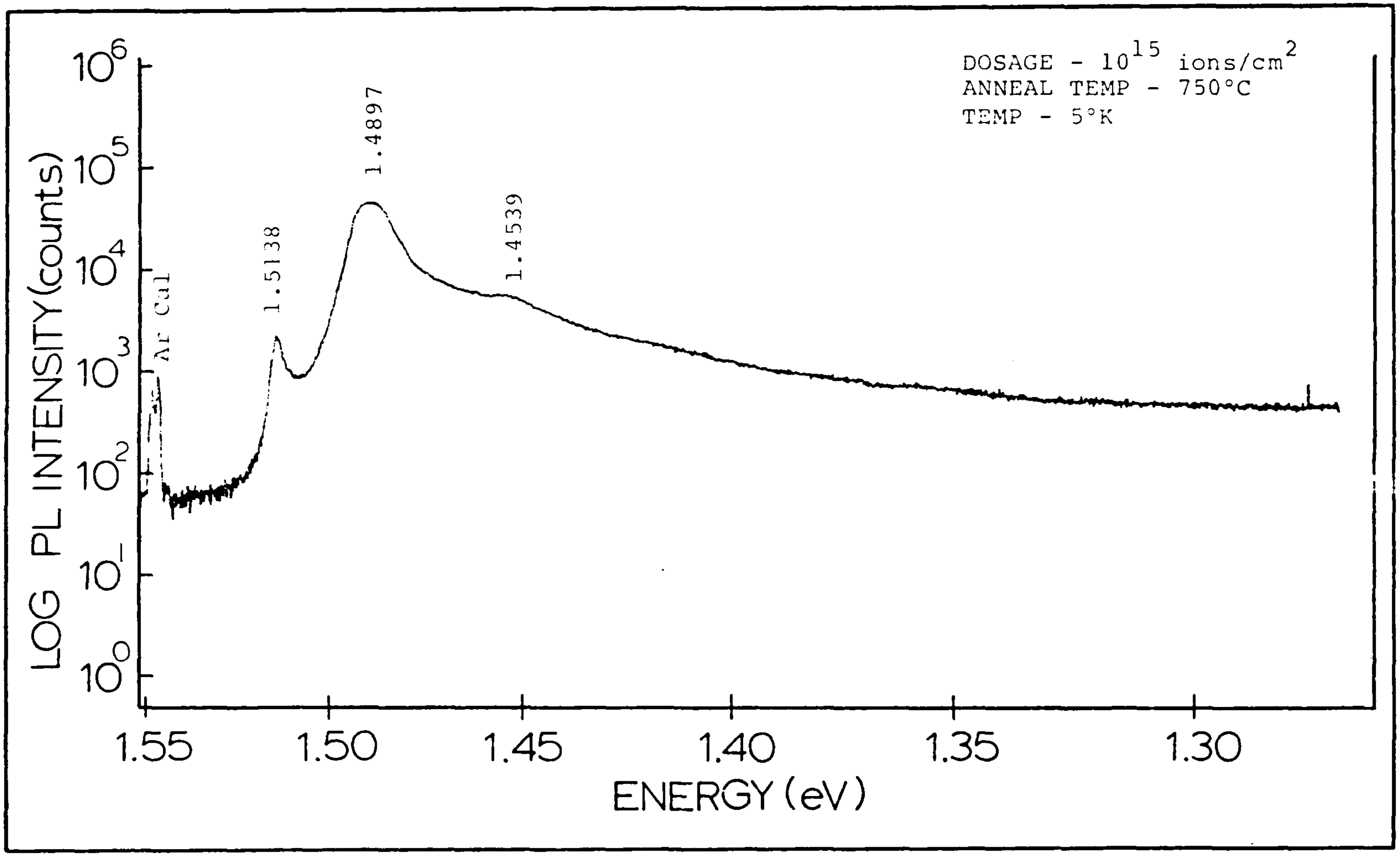

Fig. 21. PL of Sample 14

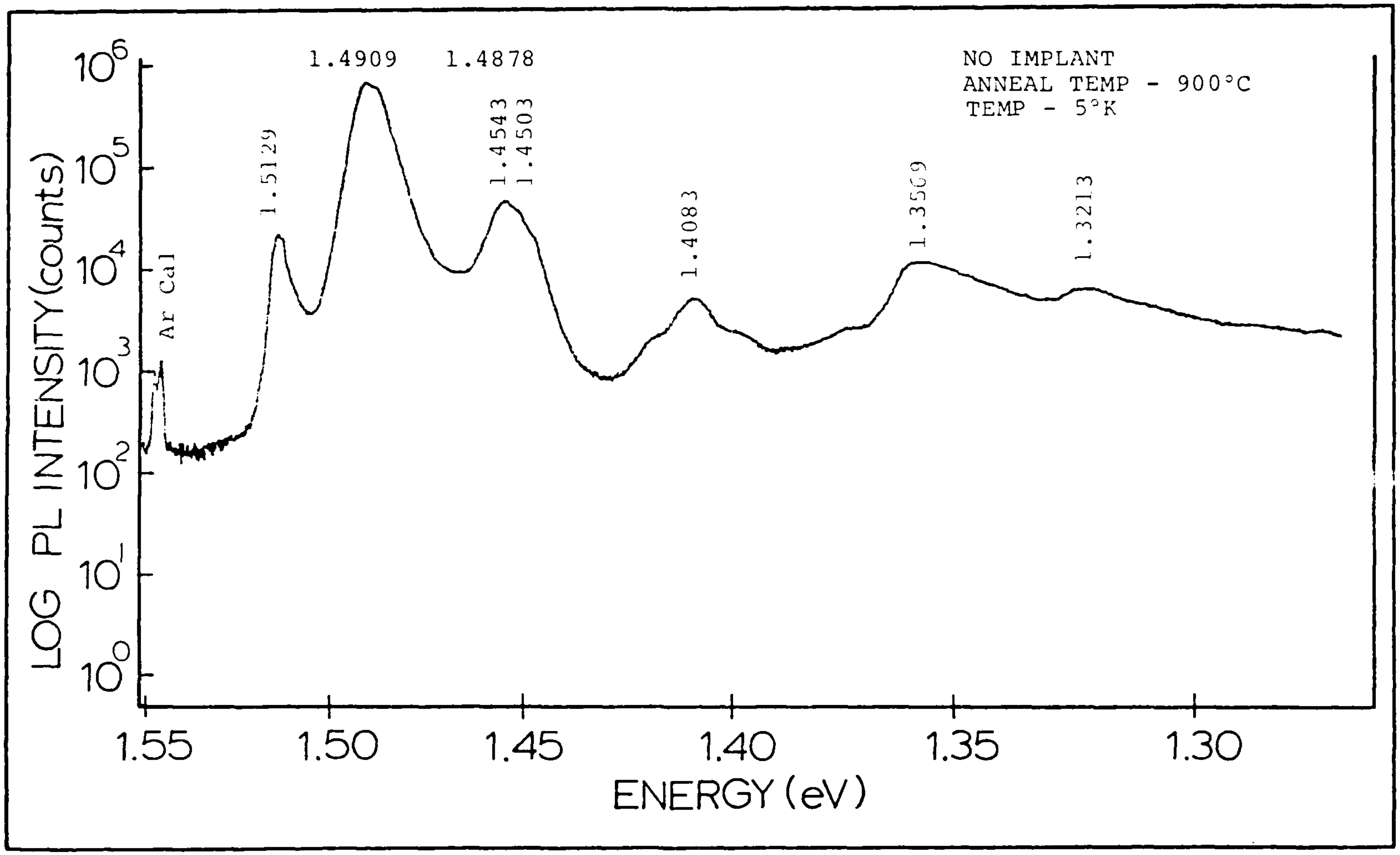

Fig. 22. PL of Sample 3

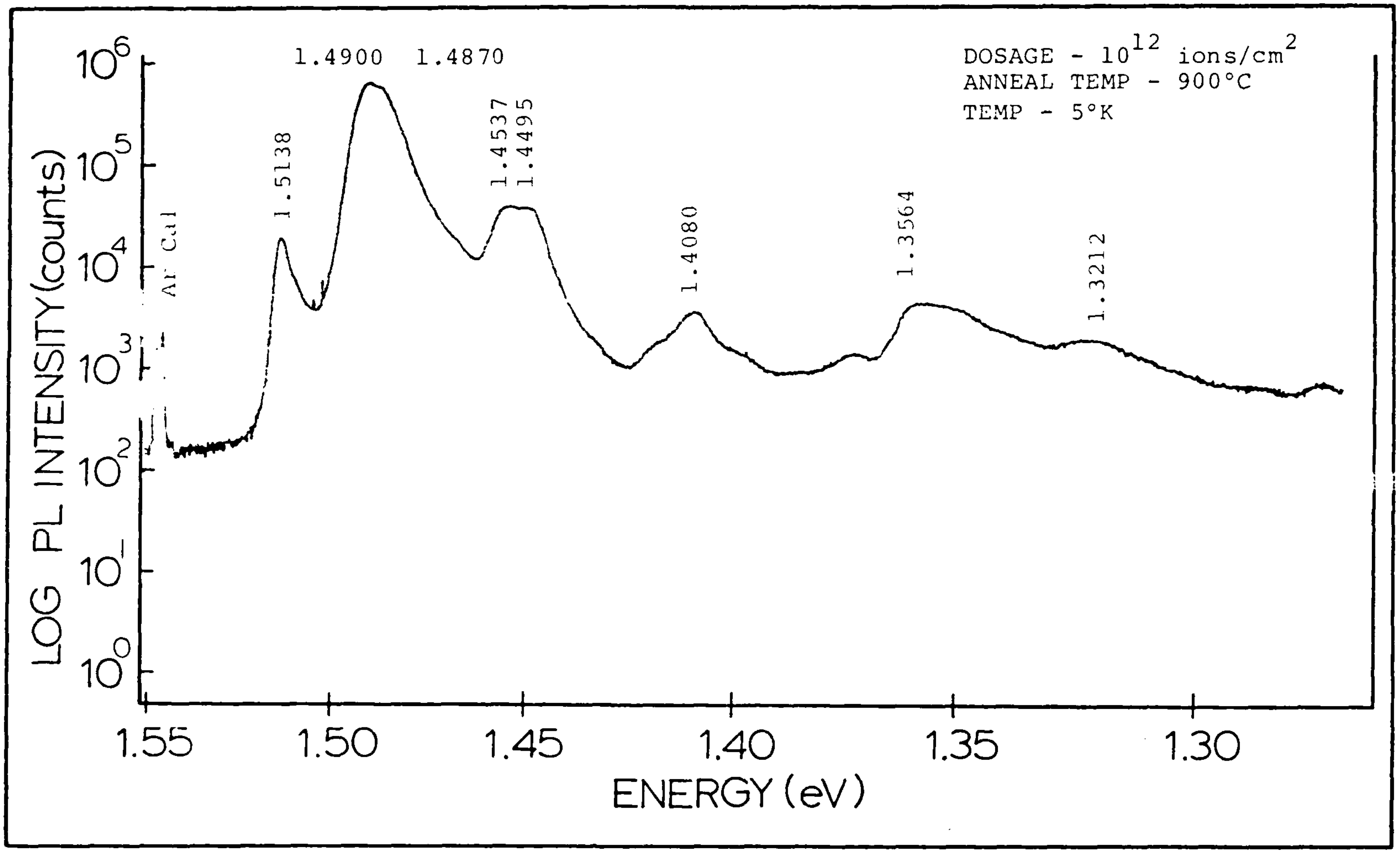

Fig. 23. PL of Sample 6

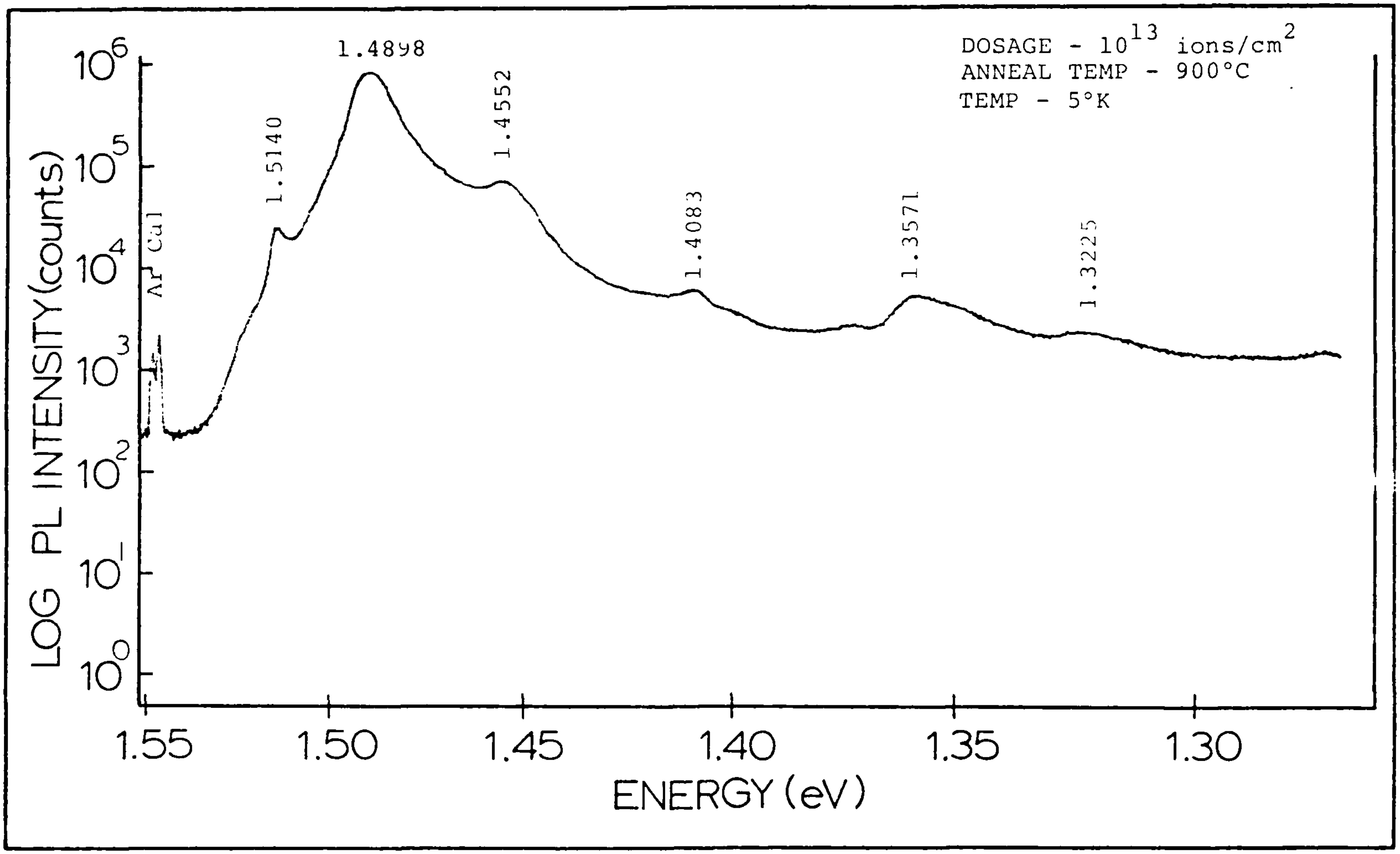

Fig. 24. PL of Sample 9

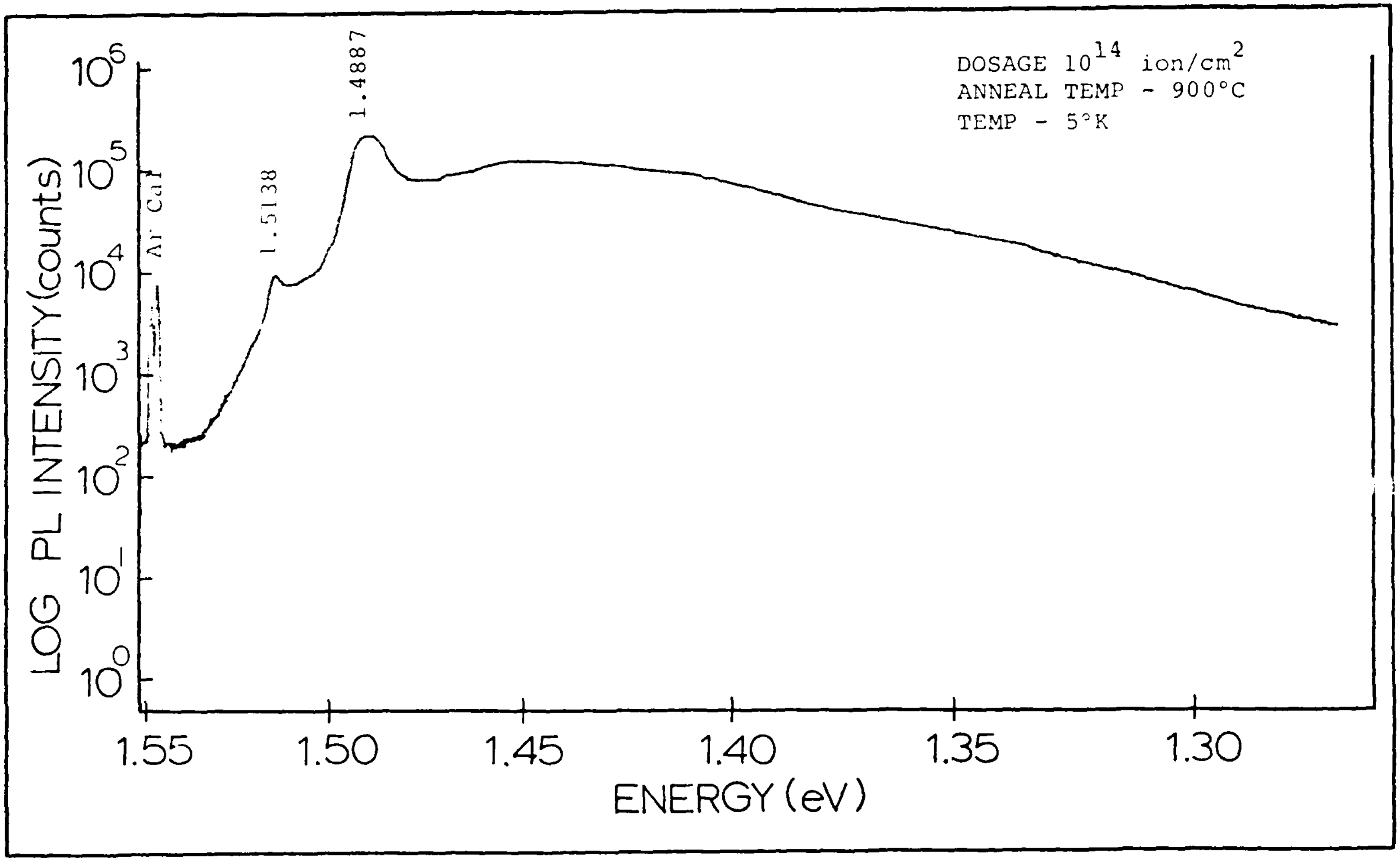

Fig. 25. PL of Sample 12

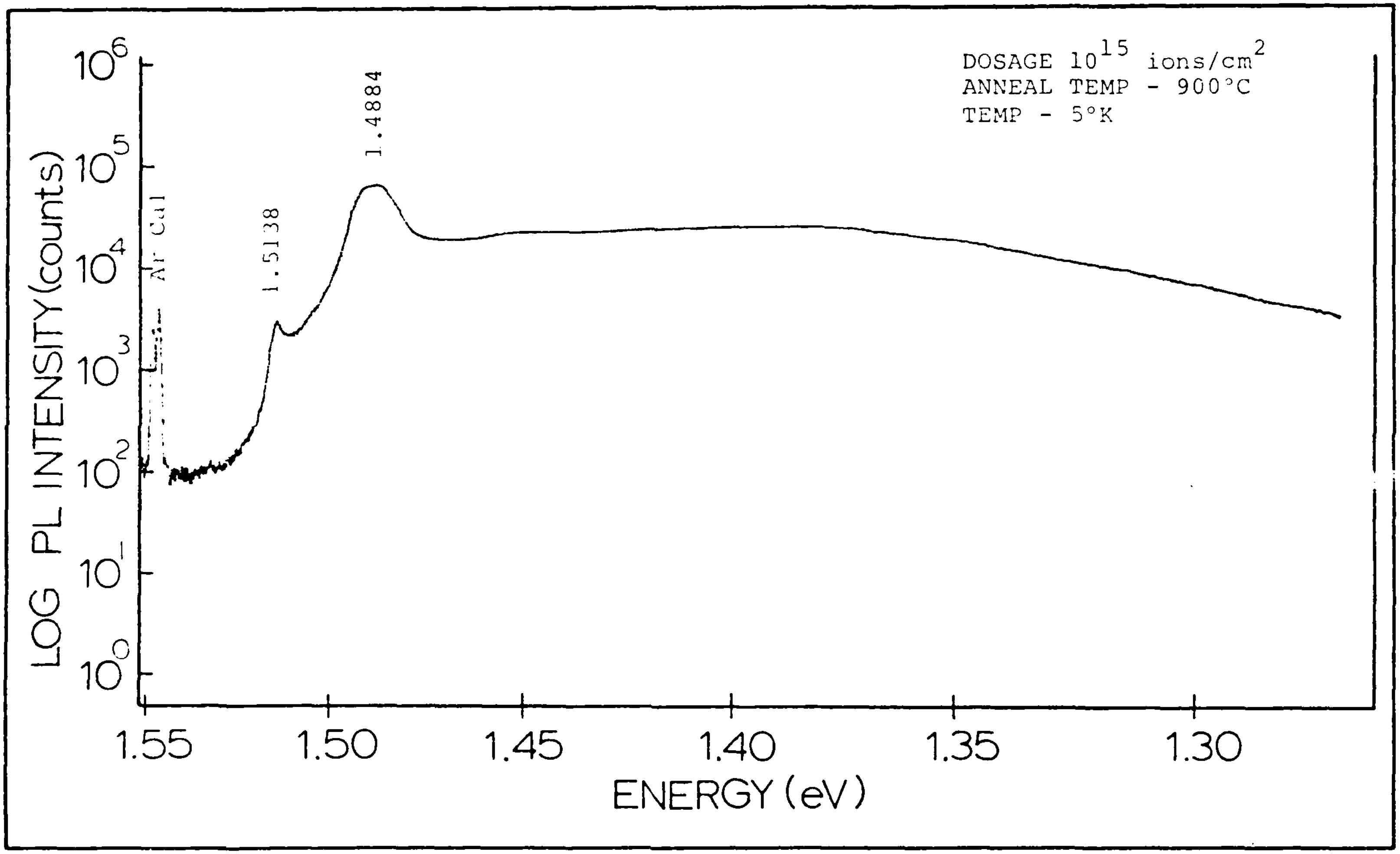

Fig. 26. PL of Sample 15

Vita

Manuel Vincent Key was born on 6 December 1946 in Caracas, Venezuela, the son of Edward and Margaret Key. He received his high school education at Riverside Military Academy in Gainesville, Georgia and graduated in 1964. After attending Georgia Southern College for three years, he transferred to Auburn University, where he received his Bachelor of Science in Electrical Engineering degree in 1972, along with a reserve commission in the United States Air Force. Upon entering active duty in 1972, he was assigned to the Air Force Weapons Laboratory in Kirtland AFB, New Mexico. In 1973 he was selected to attend Undergraduate Navigator Training at Mather AFB, California. After receiving his wings in 1974, he completed Navigator Bombadier Training and was assigned as a B-52H radar navigator to the 449th Bombardment Wing, Kincheloe AFB, Michigan. While there he became an instructor and an evaluator, and in 1977 he was assigned to the 28th Bombardment Wing, Ellsworth AFB, South Dakota. There he performed duties as an instructor and flight examiner until his assignment to the School of Engineering, Air Force Institute of Technology in June 1980.

Permanent Address: Auburn, Alabama

REPORT DOCUMENTATION PAGE

READ INSTRUCTIONS
BEFORE COMPLETING FORM

1. REPORT NUMBER
AFIT/GEO/PH/81-2

2. GOVT ACCESSION NO.
AD A1

3. RECIPIENT'S CATALOG NUMBER

4. TITLE (and Subtitle)
PHOTOLUMINESCENCE STUDY OF ION
IMPLANTATION DAMAGE IN GALLIUM ARSENIDE

5. TYPE OF REPORT & PERIOD COVERED
Master's Thesis

6. PERFORMING ORG. REPORT NUMBER

7. AUTHOR(s)
Manuel V. Key
Captain USAF

8. CONTRACT OR GRANT NUMBER(s)

9. PERFORMING ORGANIZATION NAME AND ADDRESS
Air Force Institute of Technology (AFIT/EN)
Wright-Patterson AFB, Ohio 45433

10. PROGRAM ELEMENT, PROJECT, TASK AREA & WORK UNIT NUMBERS

11. CONTROLLING OFFICE NAME AND ADDRESS
Air Force Avionics Laboratory (AFWAL/AADR)
Wright-Patterson AFB, Ohio 45433

12. REPORT DATE
December 1981

13. NUMBER OF PAGES
73

14. MONITORING AGENCY NAME & ADDRESS (if different from Controlling Office)

15. SECURITY CLASS. (of this report)
UNCLASSIFIED

15a. DECLASSIFICATION/DOWNGRADING SCHEDULE

16. DISTRIBUTION STATEMENT (of this Report)

Approved for public release; distribution unlimited

17. DISTRIBUTION STATEMENT (of the abstract entered in Block 20, if different from Report)
[illegible]

18. SUPPLEMENTARY NOTES

APPROVED FOR PUBLIC RELEASE; IAW AFR 190-17
Fredric C. Lynch 28 JAN 1982
FREDRICK C. LYNCH, Major, USAF
DIRECTOR OF PUBLIC AFFAIRS

19. KEY WORDS (Continue on reverse side if necessary and identify by block number)

ION IMPLANTATION
GALLIUM ARSENIDE
PHOTOLUMINESCENCE
III-V COMPOUNDS

20. ABSTRACT (Continue on reverse side if necessary and identify by block number)

The 5° photoluminescence (PL) from 1.55 eV to 1.36 eV of semi-insulating bulk GaAs implanted with Si was observed, using the 488 nm line of an argon-ion laser. Implant dosages were 10^{12}, 10^{13}, 10^{14}, and 10^{15} ions/cm^2. Separate sets of samples were annealed at 750°C and 900°C. The virgin unannealed sample spectrum contained a shallow donor peak at 1.513 eV, a carbon donor-to-carbon acceptor peak at 1.490 eV, a possible carbon donor-to-zinc acceptor peak at 1.487 eV, and an optical phonon peak at 1.454 eV. The virgin annealed sample spectra included, additionally, a vacancy complex-to-silicon acceptor peak at 1.406 eV, a Ga vacancy complex peak at 1.358 eV and a phonon replica at 1.322 eV. The spectra of the implanted unannealed samples showed an increasing quenching of native peaks with increasing dosage, and included no new damage related peaks. The spectra of the implanted samples showed an increase in the native peaks due to annealing but not due to Si dosage increases. The increase in Si dosage caused an increase in low energy broad peaks. A temperature study (5°K to 77°K), and chemical etching depth resolved study of a sample implanted with 10^{15} ions/cm^2 and annealed at 900°C showed two broad peaks: one near 1.38 eV and one near 1.42 eV. The peaks were seen to vary inversely with temperature in amplitude only; but as etch depth increased, the amplitudes increased then decreased, finally disappearing at an etch depth of 0.2 microns. The peaks were attributed to complex centers associated with Si in As sites and As vacancies. A similar study using chemical etching followed by a measurement of normalized PL of the 1.49 eV peak in the unannealed samples, showed that the PL was not restored to that of the virgin sample until nearly twice the damage depth predicted by LSS theory was reached. This was attributed to the diffusion of defects during the room temperature implantation process.

FILMED

3-8